

12-2011

BMP-SIGNALING REGULATES A COMMON TRANSCRIPTIONAL PROGRAM TO CONTROL FACIAL FORM AND SKELETAL MORPHOGENESIS

Margarita Bonilla-Claudio

Follow this and additional works at: https://digitalcommons.library.tmc.edu/utgsbs_dissertations



Part of the [Medicine and Health Sciences Commons](#)

Recommended Citation

Bonilla-Claudio, Margarita, "BMP-SIGNALING REGULATES A COMMON TRANSCRIPTIONAL PROGRAM TO CONTROL FACIAL FORM AND SKELETAL MORPHOGENESIS" (2011). *The University of Texas MD Anderson Cancer Center UTHealth Graduate School of Biomedical Sciences Dissertations and Theses (Open Access)*. 210.

https://digitalcommons.library.tmc.edu/utgsbs_dissertations/210

This Dissertation (PhD) is brought to you for free and open access by the The University of Texas MD Anderson Cancer Center UTHealth Graduate School of Biomedical Sciences at DigitalCommons@TMC. It has been accepted for inclusion in The University of Texas MD Anderson Cancer Center UTHealth Graduate School of Biomedical Sciences Dissertations and Theses (Open Access) by an authorized administrator of DigitalCommons@TMC. For more information, please contact digitalcommons@library.tmc.edu.

**BMP-SIGNALING REGULATES A COMMON TRANSCRIPTIONAL PROGRAM
TO CONTROL FACIAL FORM AND SKELETAL MORPHOGENESIS**

by

Margarita Bonilla-Claudio, B.S.

APPROVED:

James F. Martin, M.D., Ph.D.
Supervisory Professor

Yasuhide Furuta, Ph.D.

Mingyao Liu, Ph.D.

Pierre D. McCrea, Ph.D.

Michael R. Blackburn, Ph.D.

APPROVED:

Dean, The University of Texas
Graduate School of Biomedical Sciences at Houston

**BMP-SIGNALING REGULATES A COMMON TRANSCRIPTIONAL PROGRAM
TO CONTROL FACIAL FORM AND SKELETAL MORPHOGENESIS**

A

DISSERTATION

Presented to the Faculty of

The University of Texas

Health Science Center at Houston

and

The University of Texas

M. D. Anderson Cancer Center

Graduate School of Biomedical Sciences

in Partial Fulfillment

of the Requirements

for the Degree of

DOCTOR OF PHILOSOPHY

by

Margarita Bonilla-Claudio, B.S.

Houston, Texas

December, 2011

Dedication

I dedicate this thesis to my husband, for his love, emotional support, and encouragement to pursue new adventures, but most importantly, for giving me the opportunity to become the mother of our wonderful son, Guillermo Emmanuel. This is for both of you... my loves. Additionally, I would like to dedicate this dissertation to my parents and brothers that with their love and support made this journey even more pleasant. I would like to thank my grandparents for their love and understanding. Finally, I dedicate this work to my beloved pet-companions, Fluffy, Canelo, Mia and Lady Carolina.

Acknowledgments

I want to acknowledge with great appreciation, several people whose involvement and support made it possible to complete this project. Foremost, I want to thank my thesis mentor, Dr. James F. Martin, for providing me with the scientific foundation on which I am building my future career. All past and present members of my advisory, examining and supervisory committees: Dr. Michelle C. Barton, Dr. Michael R. Blackburn, Dr. Richard R. Behringer, Dr. Yasuhide Furuta, Dr. William H. Klein, Dr. Mingyao Liu, Dr. Pierre D. McCrea and Dr. Jill M. Schumacher. The intellectual guidance, support, and assistance that they provided me, as student, made it possible for me to succeed.

I am extremely thankful for the support and help provided to me by the Martin lab family (past and present) throughout my training. I thank (in no specific order): Dr. Jennifer Selever, Dr. Lijiang Ma, Dr. Feiyan Dong, Dr. Di Ai, Dr. Zheng Huang, Dr. Xiaoxiao Sun, Dr. Jun Wang, Yan Bai, Min Zhang, Dr. Todd R. Heallen, Dr. Ye Tao, Dr. Stephanie B. Greene, Dr. Mei-Fang Lu, Thuy T. Tran and, Elzbieta A. Klysik.

I am very grateful for all of the wonderful friendships that I have gained during these years: Maria Rodriguez, Luis Machado, Yasmine Valentin, Joel Otero, Nilsa Rivera, Jose Anibal Torres, Wilfredo Cosme, Jessica De Orbeta, Tania Rodriguez, Gabriel Villares, Ivone Bruno, Guermarie Velazquez, Enrique Fuentes, Zobeida Cruz, Nilza Biaggi, Juan Crespo and Yanira Berrios.

Abstract

BMP-SIGNALING REGULATES A COMMON TRANSCRIPTIONAL PROGRAM TO CONTROL FACIAL FORM AND SKELETAL MORPHOGENESIS

Publication No. _____

Margarita Bonilla-Claudio, B.S.

Supervisory Professor: James F. Martin, M.D., Ph.D.

Much of the craniofacial skeleton, such as the skull vault, mandible and midface, develops through direct, intramembranous ossification of the cranial neural crest (CNC) derived progenitor cells. Bmp-signaling plays critical roles in normal craniofacial development, and Bmp4 deficiency results in craniofacial abnormalities, such as cleft lip and palate. We performed an in depth analysis of *Bmp4*, a critical regulator of development, disease, and evolution, in the CNC. Conditional *Bmp4* overexpression, using a tetracycline regulated *Bmp4* gain of function allele, resulted in facial form changes that were most dramatic after an E10.5 *Bmp4* induction. Expression profiling uncovered a signature of Bmp4 induced genes (BIG) composed predominantly of transcriptional regulators controlling self-renewal, osteoblast differentiation, and negative Bmp autoregulation. The complimentary experiment, CNC inactivation of *Bmp2*, *Bmp4*, and *Bmp7*, resulted in complete or partial loss of multiple CNC derived skeletal elements revealing a critical requirement for Bmp-signaling in membranous bone and cartilage development.

Importantly, the BIG signature was reduced in Bmp loss of function mutants indicating similar Bmp-regulated target genes underlying facial form modulation and normal skeletal morphogenesis. Chromatin immunoprecipitation (ChIP) revealed a subset of the BIG signature, including *Satb2*, *Smad6*, *Hand1*, *Gadd45 γ* and *Gata3* that was bound by Smad1/5 in the developing mandible revealing direct, Smad-mediated regulation. These data indicate that Bmp-signaling regulates craniofacial skeletal development and facial form by balancing self-renewal and differentiation pathways in CNC progenitors.

Table of Contents

Signatures	i
Title Page	ii
Dedication	iii
Acknowledgements	iv
Abstract	v
Table of Contents	vii
List of Figures	x
List of Tables	xi
Introduction	1
Materials and Methods	8
Mouse alleles and transgenic line	9
Doxycycline administration in mice	10
Skeletal analysis	10
Alkaline phosphatase staining	11
Western blot analysis	11
Whole mount <i>in situ</i> hybridization	12
Quantitative Real Time PCR and Microarray	13
Chromatin immunoprecipitation	14
Sequence analysis	14
Results	15
<i>Bmp2</i> , <i>Bmp4</i> , and <i>Bmp7</i> deletion in cranial neural crest results in severe loss of cranial bone	16

Inducible over-expression of <i>Bmp4</i> in the CNC	20
Facial form is dramatically altered by elevated Bmp4 in CNC	24
Expression profiling uncovers transcriptional regulators that are upregulated in the mandible of <i>Bmp4</i> gain of function embryos	30
Commons target genes that are expanded in the Bmp4 OE embryos are also downregulated in Bmp loss of function embryos	37
Subsets of transcriptional regulators are direct <i>Bmp4</i> targets	37
Discussion	41
Direct Bmp target genes regulate cranial neural crest progenitor self-renewal	42
Bmp promotes osteoblast differentiation from CNC progenitors	44
Bmp-regulated negative feedback loops are critical for mandible development	45
Bmp-signaling controls expression of multiple families of transcriptional regulators	46
Future direction	47
Appendix	49
1. <i>Bmp2</i> , <i>Bmp4</i> , and <i>Bmp7</i> conditional null alleles	50
2. Primers sequence for qRT-PCR and ChIP experiments	51
3. List of statistically significant genes that were differentially	

expressed in the mandible after <i>Bmp4</i> over-expression	52-57
Bibliography	58
Vita	69

List of Figures

Figure 1. Formation and migration of the cranial neural crest	3
Figure 2. Origin of the skeletal elements of the skull	4
Figure 3. Defects in osteoblast maturation in the absence of <i>Bmp4</i>	17
Figure 4. Increased severity of craniofacial defects in Bmp compounds mutants	18
Figure 5. Bmp4 and Bmp2 are the major ligands in frontal bone development	19
Figure 6. A tetracycline regulated <i>Bmp4</i> gain of function allele	23
Figure 7. Overexpression of <i>Bmp4</i> using doxycycline regulated system	26
Figure 8. Morphological changes in the craniofacial region after <i>Bmp4</i> over-expression	27
Figure 9. Defective cranial bone ossification in the Bmp4 OE embryos	28
Figure 10. <i>Bmp4</i> OE embryos exhibit an expansion of the facial cartilage	29
Figure 11. Differentially expressed genes in <i>Bmp4</i> OE mandibles	31
Figure 12. <i>Bmp4</i> gain of function in the neural crest cells leads to up-regulation of different transcriptional regulators	32
Figure 13. Expanded expression pattern of the BIG signature after <i>Bmp4</i> induction	34
Figure 14. Expression patterns of up-regulated genes in <i>Bmp4</i> OE embryos	35
Figure 15. Bmp deficiency results in reduced expression of Bmp-regulated	36
Figure 16. Smad-mediated regulation of a subset of Bmp-induced genes	30-40

List of Tables

Table 1. Bmp compounds mutant defects in the skeletal elements of the skull ...	21
----------------------------------------------------------------------------------------	----

Introduction

The cranial neural crest (CNC) cells are a migratory cell population that originates from the dorsal neural tube during neurulation (Fig. 1 A). CNC diversifies into multiple cell types including cartilage, bone, smooth muscles, neurons, glia, and connective tissues of the blood vessels. Migration of the CNC occurs in three recognized streams, trigeminal, hyoid, and post-otic (Fig. 1 B). Each stream has been traced from their origin to their final fate. CNC arising from rhombomers 1 and 2, forms the trigeminal ganglion neurons and craniofacial components, including the mandible. Meanwhile, CNC originating from rhombomere 4 give rise to neurons of the proximal facial ganglion and hyoid skeleton. Lastly, CNC originating from rhombomere 6 and 7 forms neurons of the proximal jugular ganglia and pharyngeal arches skeletal components (Graham et al., 2004).

Much of the craniofacial skeleton components, including the skull vault or calvarium, mandible, and midface develops through direct, intramembranous ossification of CNC-derived progenitor cells (Fig. 2) (Chai and Maxson, 2006). For example, in the skull, osteogenesis occurs at discrete areas within the cranial mesenchyme resulting in the flat bones of the skull forming between the central nervous system (CNS) and overlying ectoderm (Jiang et al., 2002). The mandible and most midfacial bones develop by direct ossification of CNC-derived branchial arch mesenchyme (Nie et al., 2006).

The complexity of neural crest cell formation involves a number of key signaling regulators, such as those mediated by the Wnt, Fibroblast growth factor

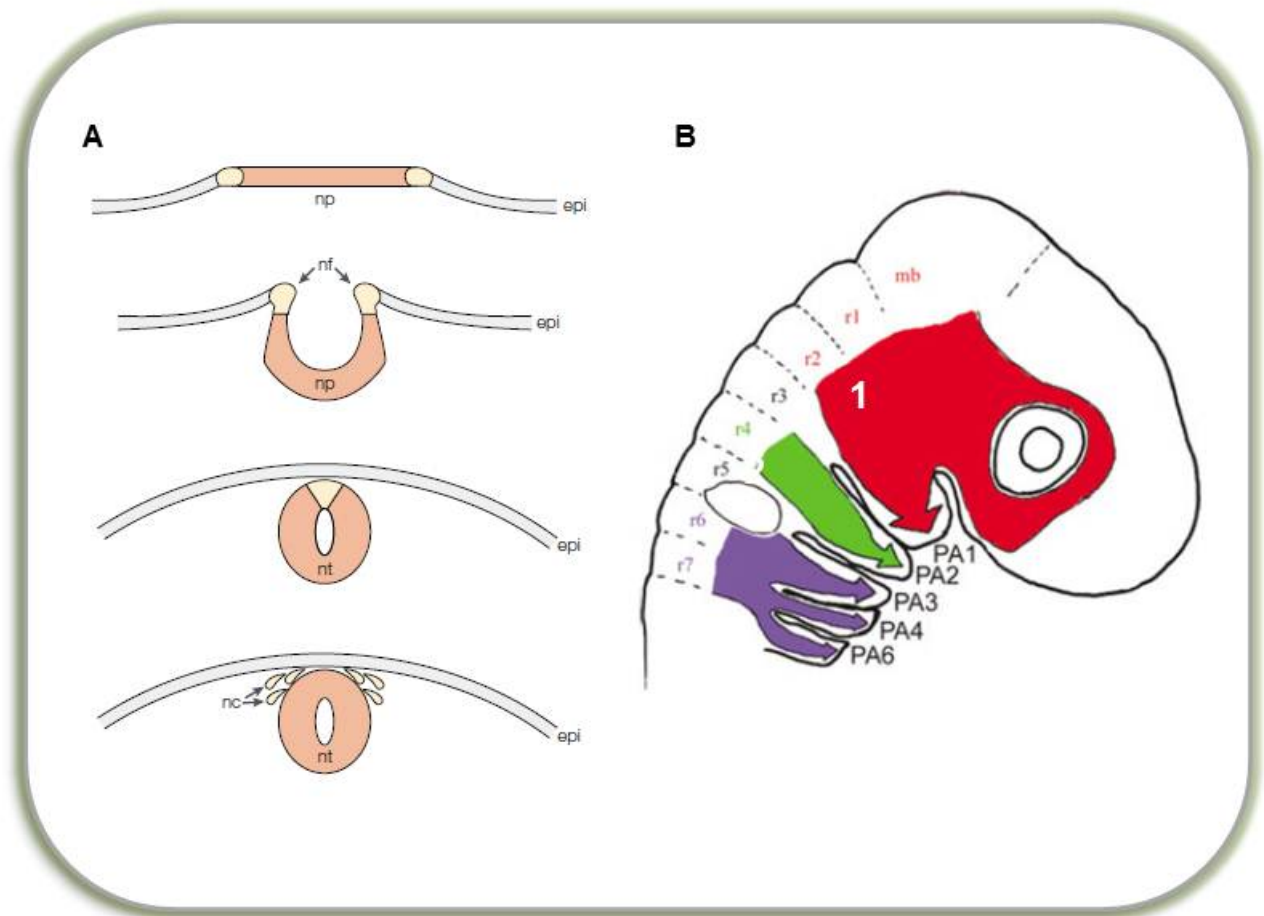


Figure 1. Formation and migration of the CNC.

(A) CNC is induced at the neural plate border. After neurulation, delamination of cells between the ectoderm and the dorsal neural tube give rise to CNC (Knecht and Bronner-Fraser, 2002). (B) Migration of the CNC occurs in three recognized streams, trigeminal (red), hyoid (green), and post-otic (purple) (Graham et al., 2004).

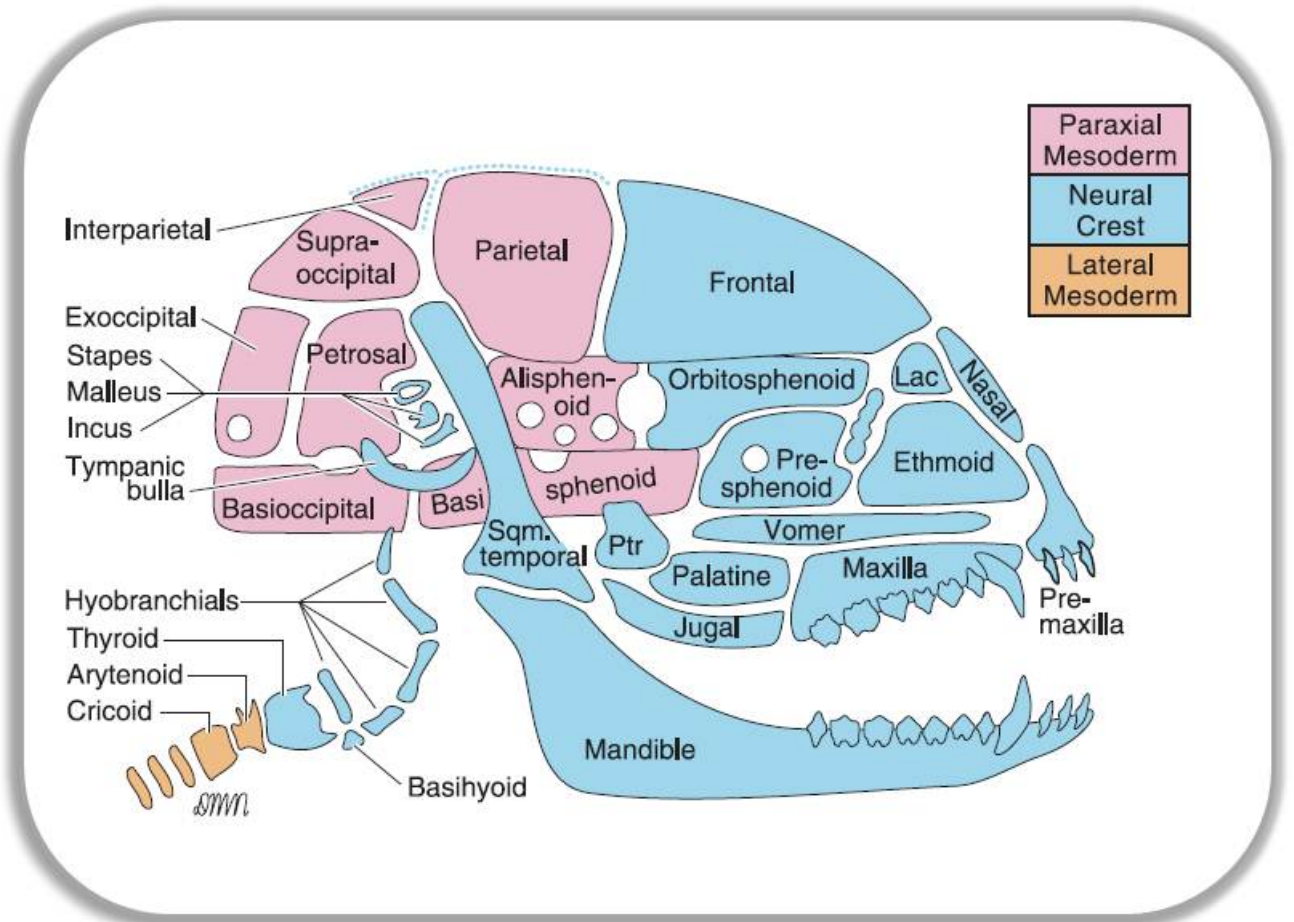


Figure 2. Origin of the skeletal elements of the skull.

Adult mouse skull showing the CNC- and mesoderm- derived bones (Noden and Trainor, 2005).

(Fgf) and Bone morphogenic protein (Bmp) pathways (Knecht and Bronner-Fraser, 2002). For example, studies have shown the importance of Bmp-signaling in the specification of the neural plate and neural crest cells (Tribulo et al., 2003). Furthermore, migration of the CNC cells to the facial primordia also involves the participation of Bmp-mediated signaling. Inhibition of Bmp2 and Bmp4 in the CNC results in hypomorphic branchial arches, while neural and skeletal derivatives did not develop (Kanzler et al., 2000).

Bmp-signaling plays a critical role in normal craniofacial development. Several studies have elegantly demonstrated that *Bmp4* deficiency results in craniofacial anomalies, such as cleft lip and palate, in mouse and humans (Liu et al., 2005b; Suzuki et al., 2009). In the mandible, *Bmp4* has been shown to regulate proximo-distal patterning and timing of bone differentiation in mandibular mesenchyme (Liu et al., 2005a; Merrill et al., 2008). There is strong evidence that Bmp-signaling regulates craniofacial morphologic change during evolution. Both gain of function studies and comparative expression data revealed *Bmp4* to be a critical regulator of beak shape in Darwin's finches, a classic model of evolutionary diversification (Abzhanov et al., 2004; Wu et al., 2004). Other experiments in Cichlid fish also support the notion that *Bmp4* is a major regulator of craniofacial cartilage shape and morphologic adaptive radiation (Albertson et al., 2005). In summary, while the role of Bmp-signaling in craniofacial development has been well studied, the downstream genes regulated in response to Bmp-signaling remain poorly understood.

Recent molecular insights into Bmp-signaling indicate that the downstream effector mechanisms for Bmp-signaling are complex and require further study (Wang et al., 2011). The canonical Bmp pathway involves nucleo-cytoplasmic shuttling of Smad effectors in response to Bmp-signaling. Bmp, as members of the TGF family, are dimeric ligands that bind to a pair of membrane BMP receptor type I and type II (BMPRI and BMPRII). These serine/threonine kinase receptors form a hetero-tetramer receptor complex, while type II receptors can phosphorylate type I receptors at the cytoplasmic region. Upon phosphorylation, a docking site is created that enables receptor-regulated Smad proteins (Smad1, Smad5 and Smad8) binding and further activation (Massague et al., 2005). Phosphorylated receptor-regulated Smad protein can then associate with Smad4 and form a heterodimer complex capable of regulating gene expression (Nohe et al., 2004).

In addition, several studies have shown that Smad-independent mechanisms mediated through MAPK pathways, can play an important role in tooth development (Xu et al., 2008). More recent work, uncovered a third Bmp effector mechanism, revealing that Smad1/5 can directly bind to the Drosha complex to promote microRNA (miR) processing (Davis et al., 2008). Furthermore, our group has shown that Bmp-signaling can induce miR transcription through a canonical Smad regulated mechanism (Wang et al., 2010). Despite the central importance of Bmp signaling for craniofacial development, congenital defects, and evolution, the mechanisms underlying Bmp action in CNC remains poorly understood.

In this study, we investigated Bmp signaling in CNC development using both gain and loss of function approaches. Inactivation of *Bmp2*, *Bmp4*, and *Bmp7* in

CNC indicate that *Bmp2* and *Bmp4* are the major Bmp ligands required for development of CNC-derived bone and cartilage. Moreover, gain of function studies indicate that elevated *Bmp4* in CNC results in dramatic changes in facial shape. Expression profiling and quantitative RT-PCR (qRT-PCR) studies uncovered a common set of Bmp-regulated target genes in both gain and loss of function embryos. Subsets of Bmp-regulated targets were directly bound by Smad 1/5 indicating direct regulation. Our data suggest a role for Bmp-regulated genes to modulate self-renewal, osteoblast differentiation, and negative feedback regulation. Moreover, we suggest that Bmp signaling is a key player in skeletal morphogenesis and facial shape by controlling the balance between self-renewing progenitors and differentiating lineage restricted cells. Negative feedback regulation, a mechanism used to finely modulate Bmp-signaling levels, is likely a general output of Bmp-signaling in multiple contexts.

Materials and Methods

Mouse alleles and transgenic lines.

The generation and characterization of *Bmp2* and *Bmp4* conditional null mice and *Wnt1Cre* transgene mice have been previously described (Liu et al., 2004; Ma and Martin, 2005 and Chai, 2000). The conditional *Bmp7* null allele will be described elsewhere (Bai Y and Martin JF, unpublished) (Appendix 1).

To generate the *Bmp4*^{TetO} allele we constructed a targeting vector that resulted in a 665 bp deletion upstream of and including the *Bmp4* basal promoter and *Bmp4* exon 1. We modified the TetO plasmid that was a kind gift from Raymond MacDonald laboratory at The University of Texas Southwestern Medical Center. The plasmid contains the tetracycline operator (TetO7), CMV promoter, IRES-lacZ and a poly-adenylation sequence. *Bmp4* genomic DNA was isolated from the 129/S BAC library. A 9-kb EcoRI fragment of *Bmp4* genomic DNA was subcloned into pBluescript (Stratagene). We inserted *Bmp4* cDNA into NotI and KsaI sites downstream of the TetO7 and CMV promoter. The *phosphoglycerol kinase neomycin-resistance cassette (pgk-neo)* with two flanking Frt sites was blunt cloned into the AclI site downstream of the IRES-LacZ. The 3 kb 3' homology arm was amplified by PCR using the primers (5'-3') tgagcagggcaacctggagaggg and tccgaatggcactacggaatggct and blunt end ligated into SmaI site downstream of *pgk-neo*. The *Bmp4*^{TetO} 5' arm, 1.7 kb EcoRI-ApaI fragment, was cut from *Bmp4* genomic DNA and blunt end cloned into XhoI site upstream of the tetO7. The targeting construct was linearized with PmeI and electroporated into AK7 embryonic stem cells, selected in G418, and screened by Southern blot. The cells were

digested with EcoRV and *Bmp4* Exon 4 was used as the 3' flanking probe. Wild type allele gives a 22 kb EcoRV fragment and the targeted allele give a 16kb EcoRV fragment. The targeting frequency for the TetO allele is 4.2% (7/167). We also used a Spe1 digest to confirm correct targeting: the wild type band was 6.4 kb, the cDNA band was 11.7 kb, and the mutant allele was 8.0 kb. We used the Rosa 26 rtTA allele (Belteki et al., 2005) to express the reverse tetracycline activator (Tet-on) under the control of the *Wnt1*^{cre} allele. This will drive *Bmp4*^{TetO} allele expression on the neural crest cells in the presence of doxycycline.

Doxycycline administration in mice.

Pregnant females were given doxycycline (Sigma) in the drinking water (2mg/ml) and in the food (Bio-Serv; 200mg/kg), for a 24 hour period unless otherwise specified.

Skeletal analysis.

Dissected embryos were placed overnight in water and scalded in hot water for 30 seconds. The skin and internal organs were removed and the samples were fixed overnight in 95% ethanol. The cartilage was stained with 0.15mg/ml Alcian Blue (Sigma) in a 1:4 mixture of glacial acetic acid and 95% ethanol. After staining overnight, the samples were rinsed twice in 95% ethanol and incubated for 24 hrs in 95% ethanol. In preparation for bone staining, samples were placed in 2% KOH for

1 hr. Bones were stained using 0.05mg/ml of Alizarin red (Sigma) diluted in 2% KOH for 2-4 hrs and then cleared with glycerol.

Alkaline Phosphatase staining.

E14.5 embryos were dissected, decapitated and fixed in 4% paraformaldehyde for 1 hour. Heads were bisected mid-sagittally and the brain and dura mater removed, washed three times in phosphate buffered saline (PBS) and Alkaline phosphatase buffer (100mM NaCl; 100mM TrisHCl pH 9.5; 50mM $MgCl_2$; 0.1% Tween-20; 2mM Levamisole). A combination of nitro-blue tetrazolium chloride and 5-bromo-4-chloro-3'-indolylphosphate p-toluidine salt (NBT/BCIP) (Roche) substrate in Alkaline phosphatase buffer was added until bone staining was observed. Samples were then washed in PBS, and post-fixed in 4% paraformaldehyde.

Western Blot

Cell lysates were prepared by dissecting E11.5 mandibles in PBS. Tissue was then homogenized in lysis buffer (50 mmol/L Tris, 150 mmol/L NaCl, 1% Triton X-100 (Bio-Rad), 0.5% deoxycholate (Sigma) plus protease inhibitors cocktail (Roche), EDTA, and sodium vanadate (Sigma). Sample protein concentration was determined by the Protein Assay Reagent kit (Pierce). Whole cell lysates were separated by 12% SDS-PAGE and transferred to nitrocellulose. Blots were blocked with 5% nonfat milk at room temperature for 1 hour. Blots were incubated with the

p-Smad1/5/8 polyclonal antibody (1:1,000 dilution; Cell Signaling) and Smad 1/5/8/ polyclonal antibody (1:1,000 dilution; Santa Cruz) at room temperature with agitation for 1 hour, followed by incubation with anti-rabbit IgG horseradish peroxidase–conjugated antibody (1:2,000; GE Healthcare). Blots were developed using an enhanced chemiluminescence detection kit (ECL; Pierce). To confirm equal loading we used anti-β-actin antibody (1:5,000; Sigma). Western Blots were quantified by densitometry analysis using Image J software (NIH).

Whole mount *in situ* hybridization.

We thank James Douglas Engel, Richard Maas, Robert E. Maxson Jr, Sylvia Evans and Stephen E. Harris for providing Gata3, Msx1, Msx2, Tbx20 and Bmp4 *in situ* probes. Plasmids for *in situ* probes have been previously described: *Dlx6* (Charite et al., 2001), *Gata3* (Ruest et al., 2004b), *Hand1* (McFadden et al., 2005), *Smad6* (Ma et al., 2005), *Msx1* (Ishii et al., 2005), *Msx2* (Ishii et al., 2003), and *Tbx20* (Shen et al., 2011). Full-length cDNA for mouse BMP4 was provided by Dr. Stephen Harris and was linearized with *SpeI* and transcribe with T7. Exon 3 and 4, including 3'UTR of *Gadd45γ* were amplified and subcloned into T-easy vector. Plasmid was linearized with *EcoRV* and transcribe with T7 RNA polymerase. *Cux2* (exon 23) and *Satb2* (exon10) were amplified and subcloned into T-easy vector. Plasmid was linearized with *SacI* and transcribe with T7 RNA polymerase.

Whole mount *in situ* hybridization were performed as follows: embryos were fixed overnight in 10% formalin then dehydrated in 100% methanol overnight until

genotype were confirmed. Embryos were re-hydrated in a graded series of methanol/PBS-Tween and treated with 10 μ l/ml of proteinase K for 15 minutes followed by 10 minute treatment with 2mg/ml glycine. Before overnight probe hybridization at 70°C, embryos were fixed for 20 minutes with 4% paraformaldehyde. Embryos were washed and pre-blocked with 10% sheep serum before overnight incubation with anti-Digoxigenin-AP (Roche) at 4°C. Additional washes were performed with TBST before detection with NBT/BCIP (Roche). For all experiments, at least three mutants and three controls embryos were analyzed for each probe.

Quantitative Real Time PCR and Microarray.

E11.5 mandibles were dissected in cold PBS and placed in RNAlater (Ambion) for RNA stabilization. mRNA was then extracted using the RNeasy Micro Kit (Qiagen). First strand cDNA synthesis was then performed utilizing the SuperScript™ II Reverse Transcriptase kit (Invitrogen) with 500ng of mRNA. Quantitative Real-Time PCR was performed using SYBR Green QPCR Master Mix (Invitrogen) in triplicate reactions and ran on Mx3000P thermal cycler (Stratagene). Primers used in this study are listed in Appendix 2. For all qRT-PCR experiments, at least three mutants and three control embryos were analyzed. DNA microarray analysis, including gene ontology analysis, was performed using the OneArray™ Mouse Whole Genome Array (Phalanx Biotech Group). Mandibular processes were pooled to collect a minimally required RNA amount: seven Bmp4 OE and five

controls embryos were used. Gene ontology results were confirmed using DAVID Bioinformatics Resources 6.7 National Institute of Allergy and Infectious Diseases (NIAID), NIH.

Chromatin immunoprecipitation.

Chromatin immunoprecipitation (ChIP) analysis was performed as previously described (Wang et al., 2010). We used E11.5 wild type mice mandibles and the mouse osteoblastic cell line MC3T3-E1 (ATCC). Cells were maintained and propagated following ATCC protocols. Experiments were performed with 90% confluent cultures and Bmp4 (R&D System) was added to the media for a final concentration of 25pg/μl for 12hrs. Primer sequences used for amplification of the Bmp/Smad regulatory elements are found in Appendix 2.

Sequence analysis

For sequence analysis and multiple sequence alignment, Ensembl genome database and MAFFT (<http://mafft.cbrc.jp/alignment/server/>) were used.

Results

***Bmp2*, *Bmp4*, and *Bmp7* deletion in cranial neural crest results severe loss of cranial bone.**

We used the *Wnt1cre* driver and a *Bmp4* conditional null allele, *Bmp4*^{floxneo} to inactivate *Bmp4* in CNC (Chai et al., 2000; Liu et al., 2004). Intercrosses between *Wnt1cre*; *Bmp4*^{floxneo/+} with *Bmp4*^{floxneo} homozygous mice generated *Wnt1cre*; *Bmp4*^{floxneo;floxneo (f/f)} mutant embryos, hereafter called *Bmp4* CKO. Evaluation of skull preparations indicated that *Bmp4* CKO mutant newborn skulls had enlarged frontal fontanelle and subtle mandibular defects (Fig. 4 A-B). Examination of *Msx1* and *Msx2* expression, markers of preosteogenic head mesenchyme, revealed that these markers were reduced, but still present, in the *Bmp4* CKO embryos (Fig. 3 A-D). Alkaline phosphatase, a marker of both preosteoblasts and mature osteoblasts, was also reduced in the frontal bone of *Bmp4* CKO embryos, indicating a defect in the transition from pre-osteoblast to osteoblast in the *Bmp4* CKO (Fig. 3 E-F). Persistent gene expression of downstream targets of the Bmp-signaling such as *Msx* gene in *Bmp4* CKO embryos suggested that other Bmp ligands likely had overlapping functions with *Bmp4* in CNC.

To test this idea, we generated compound conditional loss of function mutants for *Bmp2*, *Bmp4*, and *Bmp7* using the *Wnt1cre* driver. Analysis of *Bmp4* and *Bmp7* compound mutants indicated that *Bmp7* failed to have a significant influence on *Bmp4* CKO mutant phenotype (Fig. 4 A-E and 5 A). In contrast, *Bmp2* deletion in the *Bmp4* CKO background resulted in significant worsening of frontal and mandibular bone phenotypes. The *Bmp2/4* CKO mutant had a drastic reduction in most CNC-derivates bones, such as the frontal and mandible (Fig. 4 F-I and 5 B).

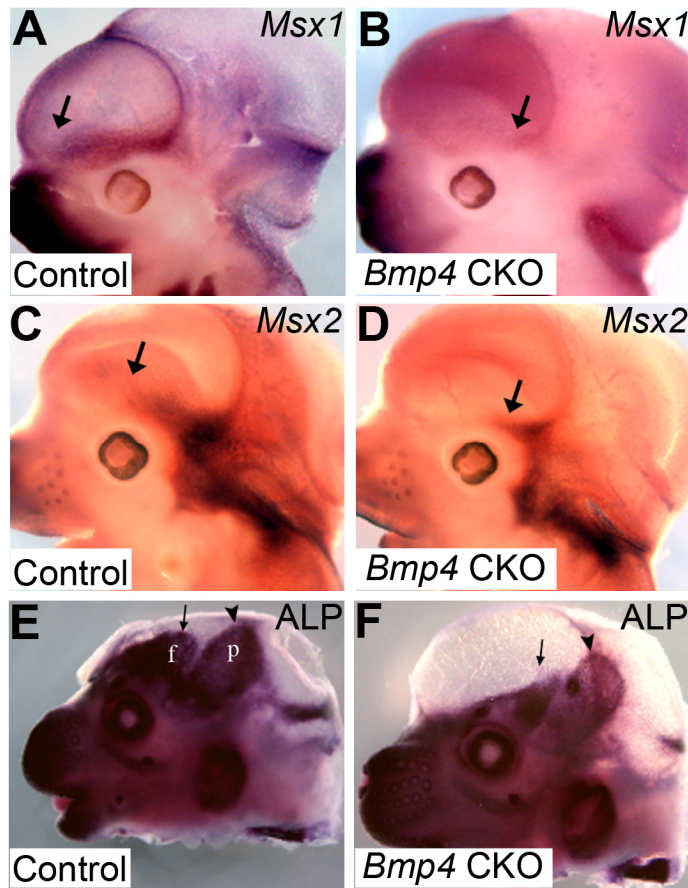


Figure 3. Defects in osteoblast maturation in the absence of *Bmp4*.

Msx1 (A-B) and *Msx2* (C-D) expression pattern in controls and *Bmp4* CKO embryos. Arrow denotes the expression of these genes in the frontal bone primordium at E12.5. The *Bmp4* CKO mutant has reduced expression of *Msx1* (B) and *Msx2* (D) in the frontal bone primordium compared to control. (E-F) Alkaline phosphatase staining of mature osteoblasts in control and *Bmp4* CKO mutant at E14.5. The *Bmp4* CKO mutant frontal bone (arrow) is extremely reduced, though the parietal bone (arrowhead) is normal when compare to control. f, frontal bone; p, parietal bone.

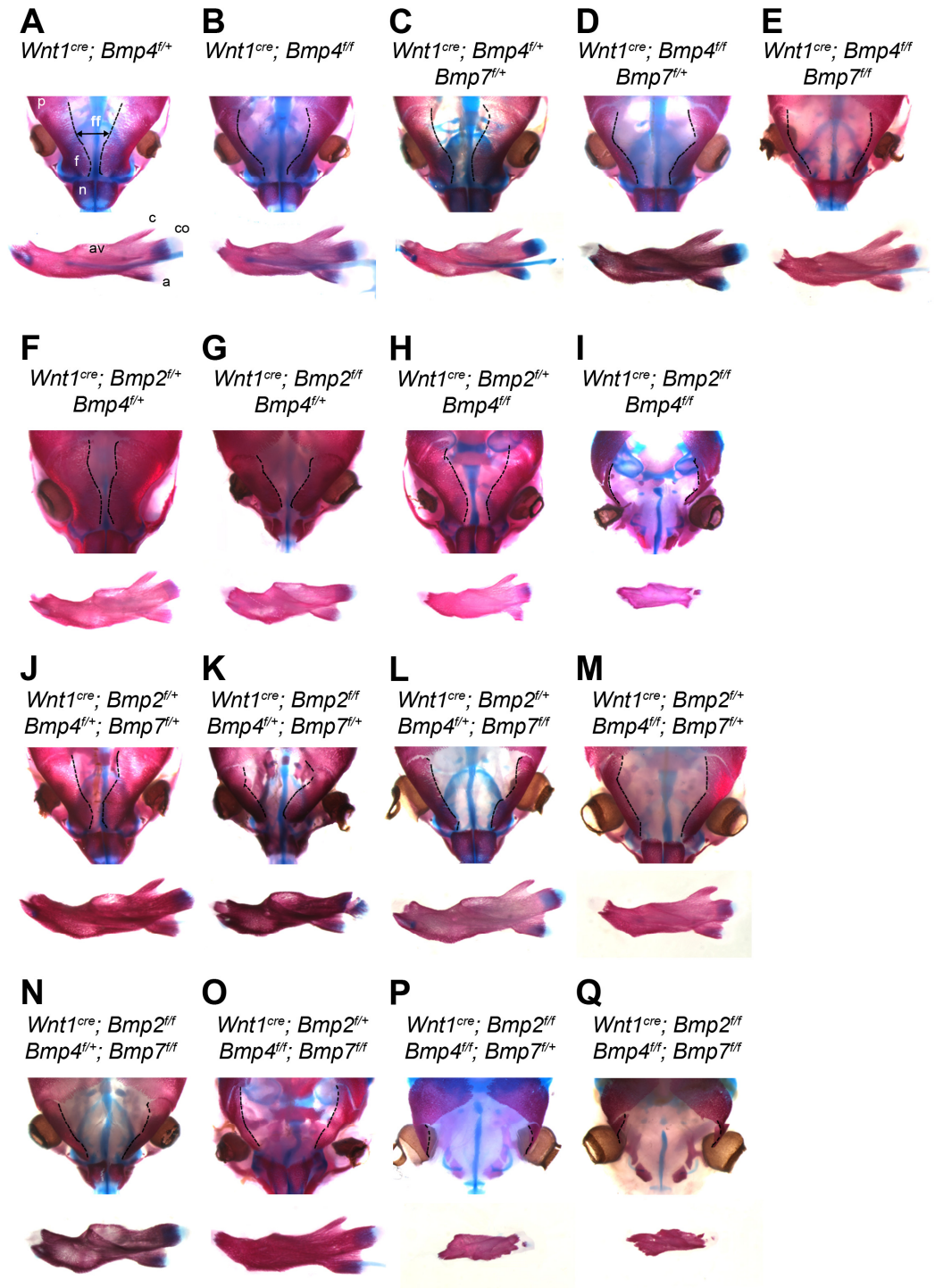


Figure 4. Increased severity of craniofacial defects in Bmp compounds mutants.

Alcian blue/alizarin red stains of E18.5 embryo showing defects in the frontal and mandible bone. Arrow indicated the distance between the frontal bones use to measure the frontal fontanelle for each genotype. a, angular process; av, alveolar bone; c, coronoid process; co, condylar process; f, frontal bone; ff, frontal fontanelle; n, nasal bone; p, parietal bone. * indicates a p-value < 0.05, error bars represent SEM.

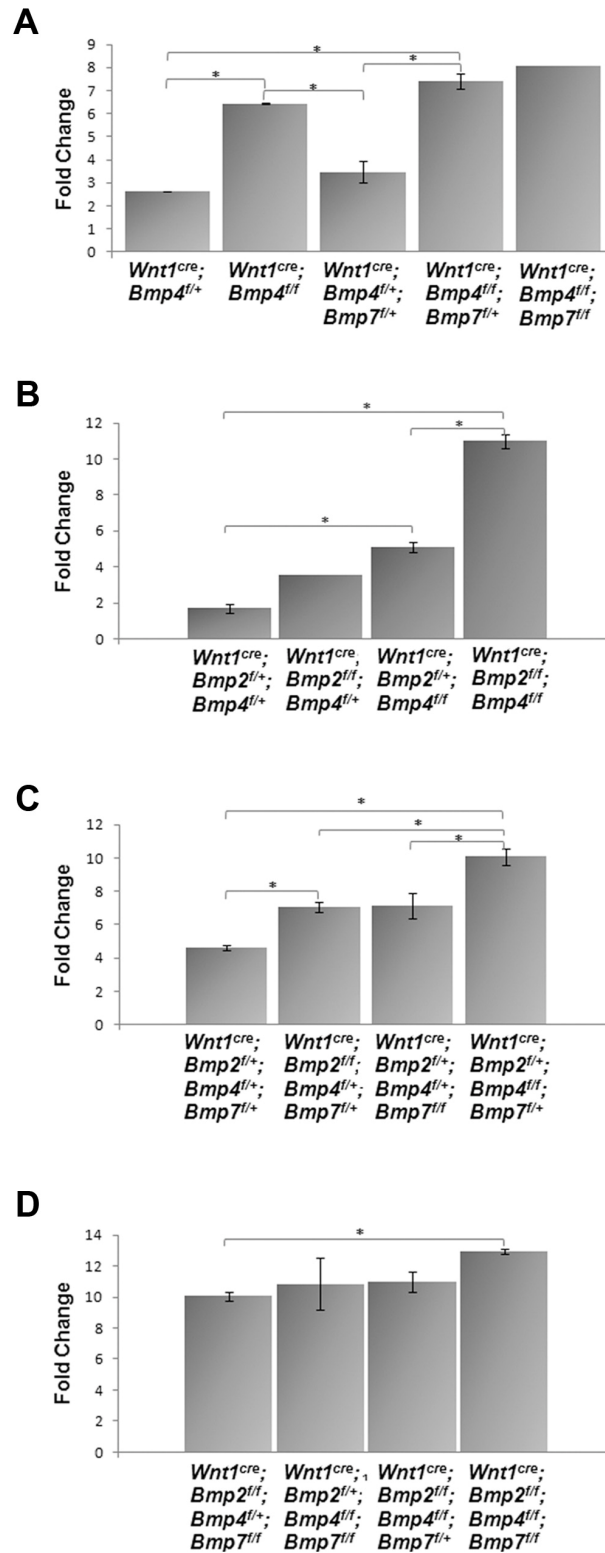


Figure 5. Bmp4 and Bmp2 are the major ligands in frontal bone development.

Bmp compounds mutants have an increase in the frontal fontanelle size when compare to littermate wildtype.

Additionally, *Bmp2* had a unique role in coronoid process development (Fig. 4 G, K, N). Analysis of triple mutant combinations further supported the conclusion that *Bmp4* and *Bmp2* were the major ligands in frontal and mandibular bone development. Comparison between embryos that were *Bmp2*; *Bmp4* compound homozygous and were either *Bmp7*^{+/+}, *Bmp7*^{flox/+} or *Bmp7*^{flox/flox} indicated that *Bmp7* has a minor role in frontal bone formation (Fig. 4 I, P and Q). In addition to the frontal and mandibular bone defects, others CNC derivative bones were affected in Bmp compound mutants (Table 1). This genetic analysis indicated that while *Bmp4* was the major functional Bmp ligand in CNC-derived bone development *Bmp2* also had important functions.

Inducible over-expression of *Bmp4* in the CNC

A bacterial based, tetracycline inducible system was used to control the expression of *Bmp4* in the cranial mesenchymal cells that give rise to the mandible and most midfacial bones (Chai and Maxson, 2006). It has been shown that with this system the induction of tetracycline, or its analog doxycycline has low basal activity, high levels of inducibility and low toxicity. In addition, multiple studies have demonstrate that tetracycline and doxycycline cross the placenta, making this system valuable for developmental studies (Gossen et al., 1995; Shin et al., 1999).

The tetracycline inducible system is a two-component system based on the *E. Coli* tet repressor. Two versions of this system exist, the original tTA and a modified

Table 1. Bmp compounds mutant defects in the skeletal elements of the skull.

Bone defects severity was scored as follows: 0, no change; 1, size reduction; 2, missing pieces and 3, missing bone.

CP: cleft palate.

Genotype	Nasal	Interparietal	Tympanic	Squamosal	Alisphenoid	Zygomatic	Maxillary	Coronoid	Condylar	Angular	Palate
Control	0	0	0	0	0	0	0	0	0	0	0
Wnt1 ^{cr9} ; Bmp4 ^{fl+}	0	0	0	0	0	0	0	0	0	0	0
Wnt1 ^{cr9} ; Bmp4 ^{flf}	0	1	0	0	0	0	0	0	0	0	0
Wnt1 ^{cr9} ; Bmp4 ^{fl+} ; Bmp7 ^{fl+}	0	0	0	0	0	0	0	0	0	0	0
Wnt1 ^{cr9} ; Bmp4 ^{flf} ; Bmp7 ^{fl+}	0	0	0	0	0	0	0	0	0	0	0
Wnt1 ^{cr9} ; Bmp4 ^{flf} ; Bmp7 ^{flf}	0	0	1	1	0	0	0	0	0	0	CP
Wnt1 ^{cr9} ; Bmp2 ^{fl+} ; Bmp4 ^{fl+}	0	0	0	0	0	0	0	0	0	0	0
Wnt1 ^{cr9} ; Bmp2 ^{flf} ; Bmp4 ^{fl+}	1	0	0	0	3	3	0	3	0	0	CP
Wnt1 ^{cr9} ; Bmp2 ^{fl+} ; Bmp4 ^{flf}	0	1	0	0	0	0	0	0	0	0	0
Wnt1 ^{cr9} ; Bmp2 ^{flf} ; Bmp4 ^{flf}	2	2	3	2	3	3	3	3	2	1	CP
Wnt1 ^{cr9} ; Bmp2 ^{fl+} ; Bmp4 ^{fl+} ; Bmp7 ^{fl+}	0	0	0	0	0	0	0	0	0	0	0
Wnt1 ^{cr9} ; Bmp2 ^{fl+} ; Bmp4 ^{fl+} ; Bmp7 ^{flf}	0	0	1	1	3	0	0	0	0	0	CP
Wnt1 ^{cr9} ; Bmp2 ^{flf} ; Bmp4 ^{fl+} ; Bmp7 ^{fl+}	1	0	0	0	3	3	0	3	0	0	CP
Wnt1 ^{cr9} ; Bmp2 ^{fl+} ; Bmp4 ^{flf} ; Bmp7 ^{fl+}	1	0	1	1	1	1	0	0	0	0	CP
Wnt1 ^{cr9} ; Bmp2 ^{flf} ; Bmp4 ^{fl+} ; Bmp7 ^{flf}	1	0	2	2	3	3	0	3	0	0	CP
Wnt1 ^{cr9} ; Bmp2 ^{fl+} ; Bmp4 ^{flf} ; Bmp7 ^{flf}	1	1	2	1	0	1	0	0	0	0	CP
Wnt1 ^{cr9} ; Bmp2 ^{flf} ; Bmp4 ^{flf} ; Bmp7 ^{fl+}	2	2	3	3	3	3	3	3	2	1	CP
Wnt1 ^{cr9} ; Bmp2 ^{flf} ; Bmp4 ^{flf} ; Bmp7 ^{flf}	2	2	3	3	3	3	3	3	3	3	CP

reverse Tet repressor, rtTA. In both systems, the tTA or rtTA fusion proteins are expressed in the cell type of interest by a tissue specific regulatory element (Gossen et al., 1995). We used a conditional reverse tetracycline transcriptional activator allele generated at Dr. Andras Nagy laboratory (Mount Sinai Hospital, Canada). The allele has an rtTA coding sequence incorporated into the Rosa 26 locus (Fig. 6 C). This allele is similar to the Rosa 26 reporter in that the rtTA is expressed only after removal of the *LoxP* flanked cassette that is dependent on cre recombinase activity (Belteki et al., 2005). In this system, rtTA protein binds to the tetracycline operator in the presence of the tetracycline analog, doxycycline (Fig. 6 C). Upon binding to the tetracycline operator (TetO), the rtTA activates transcription of the tetracycline responder transgene. This binding is not permanent and in the absence of doxycycline the transcription of the TetO responder gene stops.

To investigate the role of elevated Bmp4-signaling in CNC, we developed a tetracycline-regulated *Bmp4* allele (*Bmp4^{TetO}*) by replacing the first non-coding exon and basal promoter region of *Bmp4* with a *tet operator Bmp4* cDNA fusion gene (Figure 6 A-B). We used a cre-recombinase inducible *rtTA* (Tet-on) allele, *R26R^{rtTANagy}* allele, and the *Wnt1^{cre}* allele to induce rtTA in the CNC lineage. *Bmp4* was overexpressed by inducing *Wnt1^{cre}*; *Bmp4^{TetO}*; *R26R^{rtTANagy}* (*Bmp4* OE) embryos with doxycycline (dox).

Next, we determined whether the *Bmp4^{TetO}* allele directed significant levels of *Bmp4* expression in the CNC lineage. We treat the pregnant females with different concentration of dox in the drinking water for 24 hours. We used mandible tissue of *Bmp4* OE embryos and compared them to littermate embryos that possessed two

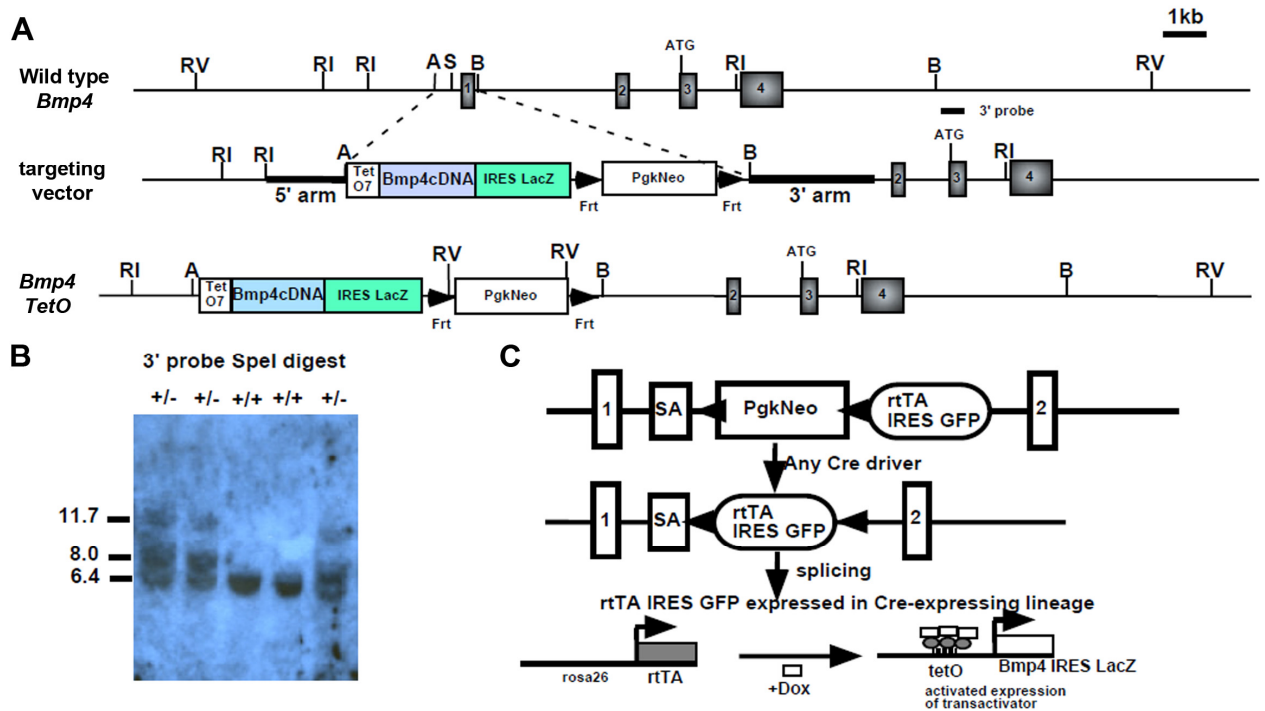


Figure 6. A tetracycline regulated *Bmp4* gain of function allele.

(A) Targeting vector of *Bmp4*^{tetO} allele, which contains the tetracycline operator (tetO7), CMV basal promoter, *Bmp4* cDNA, IRES-lacZ and *PGK-neo* resistance cassette with two flanking Frt sites, targeted in *Bmp4* basal promoter and *Bmp4* exon1. (B) Clones were screened by Southern blot, showing correct targeting by a Spe1 digestion: the wild type band was 6.4 kb, the cDNA band was 11.7 kb, and the mutant allele was 8.0 kb. (C) Schematic illustrating the strategy to regulate spatial and temporal expression of *Bmp4* using the *R26RrtTANagy* allele (Belteki et al., 2005).

wild type copies of the *Bmp4* allele (*Wnt1cre; R26R^{rtTANagy}*) as the control tissue. qRT-PCR analysis indicated that *Bmp4* OE embryos had approximately 30-fold inducible *Bmp4* upregulation. Furthermore, *Bmp4* levels were increased with higher levels of dox (Figure 7 A). We select the higher inducible dose of 2 mg/ml of dox for further experiments. Next, we want to determine how quickly our system can induce transcription of *Bmp4^{Teto}* allele. *Bmp4* induction could be detected by qRT-PCR 3 hours after dox induction and remained elevated through 24 hours of induction (Figure 7 B). Elevated *Bmp4* was also detectable in CNC by whole mount *in situ* in E10.5 embryos after 24 hours of induction (Figure 7 C). Western blot indicated that the elevated *Bmp4* mRNA expression resulted in about a 2.5-fold increase in p-Smad1/5/8 activity in the mandibular process revealing that negative regulatory mechanisms have a large impact on Bmp-signaling output (Figure 7 D). Therefore, we have been able to show that with this system we can control the spatial and temporal over-expression of *Bmp4*.

Facial form is dramatically altered by elevated Bmp4 in CNC.

We tested the phenotypic effects of elevated *Bmp4* expression in the CNC by analyzing E16.5 *Bmp4* OE embryos that had been induced at different embryonic stages. *Bmp4* inductions starting at E13.5 caused a defect in the mandible development. Mandibles were more pointed in appearance (Fig. 8 A-D), while this phenotype was intensified in the early induction (Fig. 8 D, H and L). In addition to the size reduction of the mandible, when induction started at E11.5, *Bmp4* OE

embryos showed open eyelids defects and a reduction in size of the whisker pad region (Fig. 8 E-F). The most drastic change in facial appearance was observed in *Bmp4* OE induced at E10.5. Besides the open eyelid phenotype, there was a shortening and pointed appearance in both the mandible and maxilla. These embryos show undifferentiated epithelium in which the whisker pad is not recognizable (Fig. 8 I-J). The overall shape of the head was more rounded as compared to control mouse embryo. Moreover, the orientation of the eyes was more anterior as compared to the control (Fig. 8 D, H and L). Induction at early time points resulted in open neural tube defects (data not shown). These findings indicate that increasing *Bmp4* levels regulated facial form in a stage-dependent fashion.

Skeletal preparations at E16.5 indicated that *Bmp4* induction starting at E10.5, resulted in strong reduction of rostral bony elements, such as nasal bones, with a drastically shortened face (Fig. 9 G, H). Overall bone quality was defective as revealed by multiple translucent areas in the skull bones. *Bmp4* induction at E12.5 had a less dramatic morphologic change, but the size of the nasal cartilages was expanded while nasal and frontal bones were absent or reduced (Fig. 9 E, F) and the mandible was shorter. Induction at E13.5 revealed reduction in nasal bones and coronoid process of the mandible (Fig. 9 C, D)

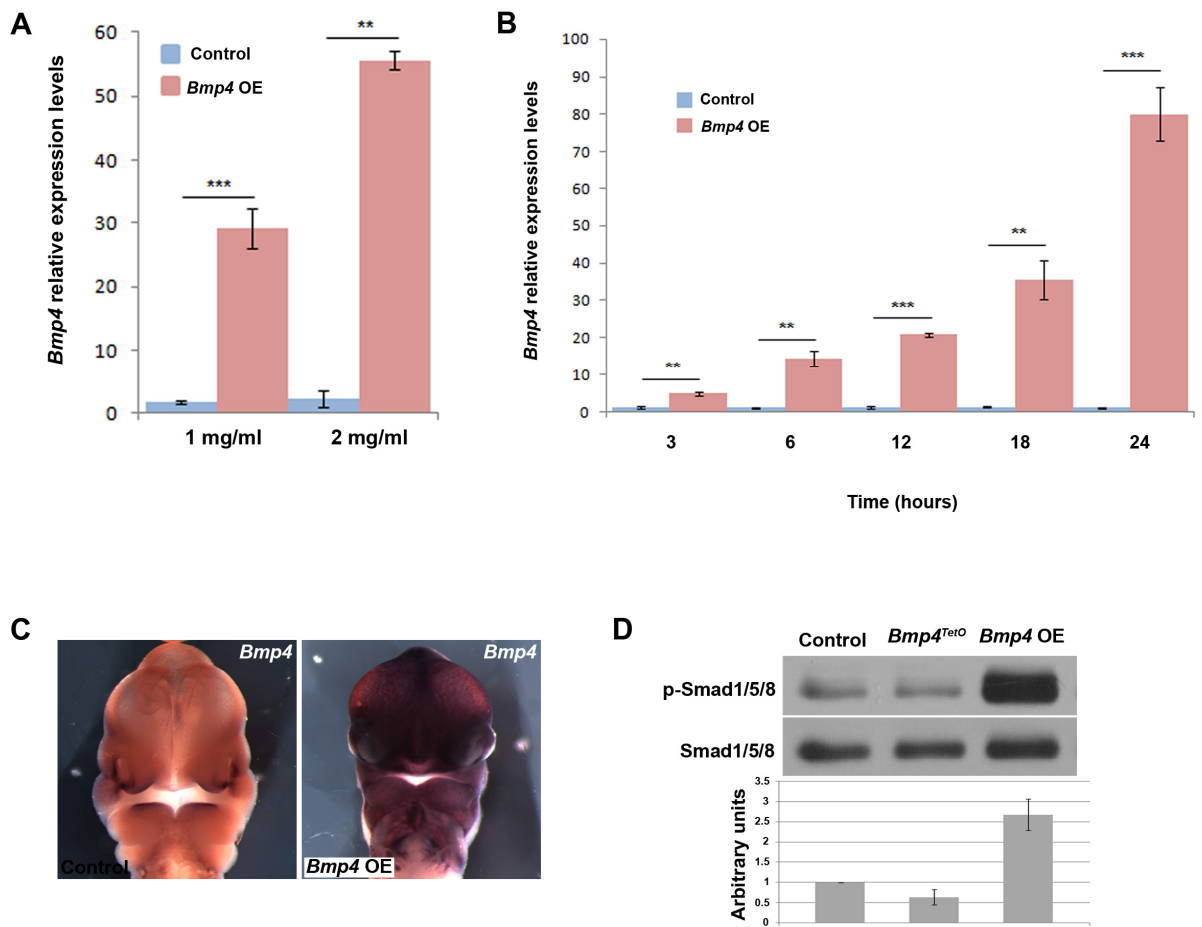


Figure 7. Overexpression of *Bmp4* using doxycycline regulated system.

(A) qRT-PCR of E11.5 mandibles showing the response of the *Bmp4*^{tetO} allele to different concentration of doxycycline. (B) qRT-PCR of E11.5 mandibles showing the response of the *Bmp4*^{tetO} allele to doxycycline at different periods of time. (C) *In situ* hybridization showing total levels of *Bmp4* transcript after 24 hrs of doxycycline (2mg/ml). (D) Western blot and densitometry (n=3) analysis of E11.5 mandibles after 24 hrs of doxycycline (2mg/ml), 10ug protein/lane. ** indicates a p-value < 0.01, *** indicates a p-value < 0.001, error bars represent SEM.

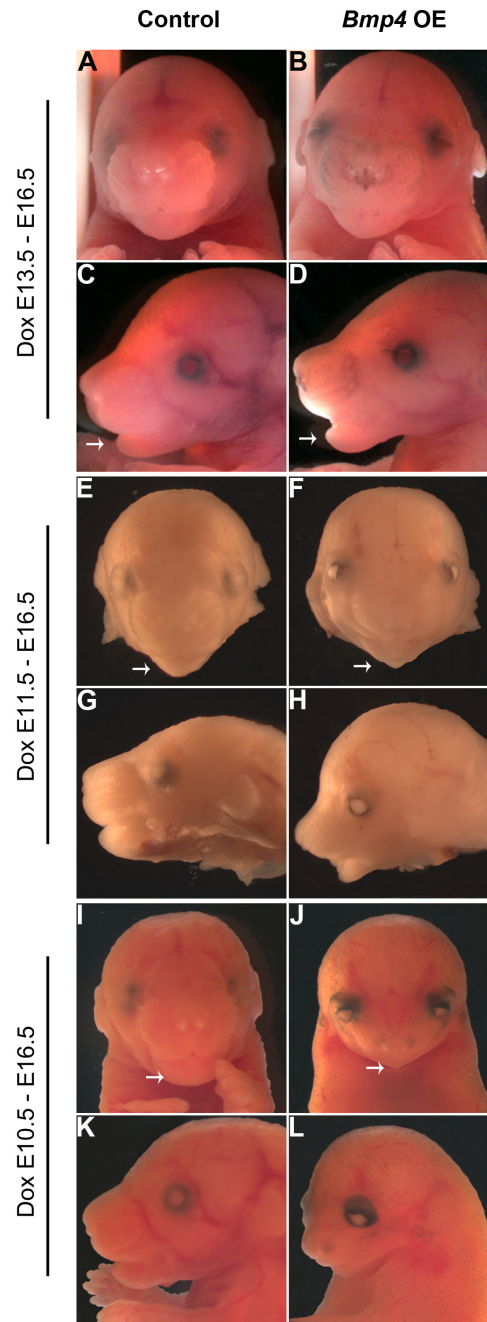


Figure 8. Morphological changes in the craniofacial region after *Bmp4* over-expression.

Frontal and lateral views of control and *Bmp4* OE embryos after the indicated induction period. Arrows point at the morphologies changes in the mandible.

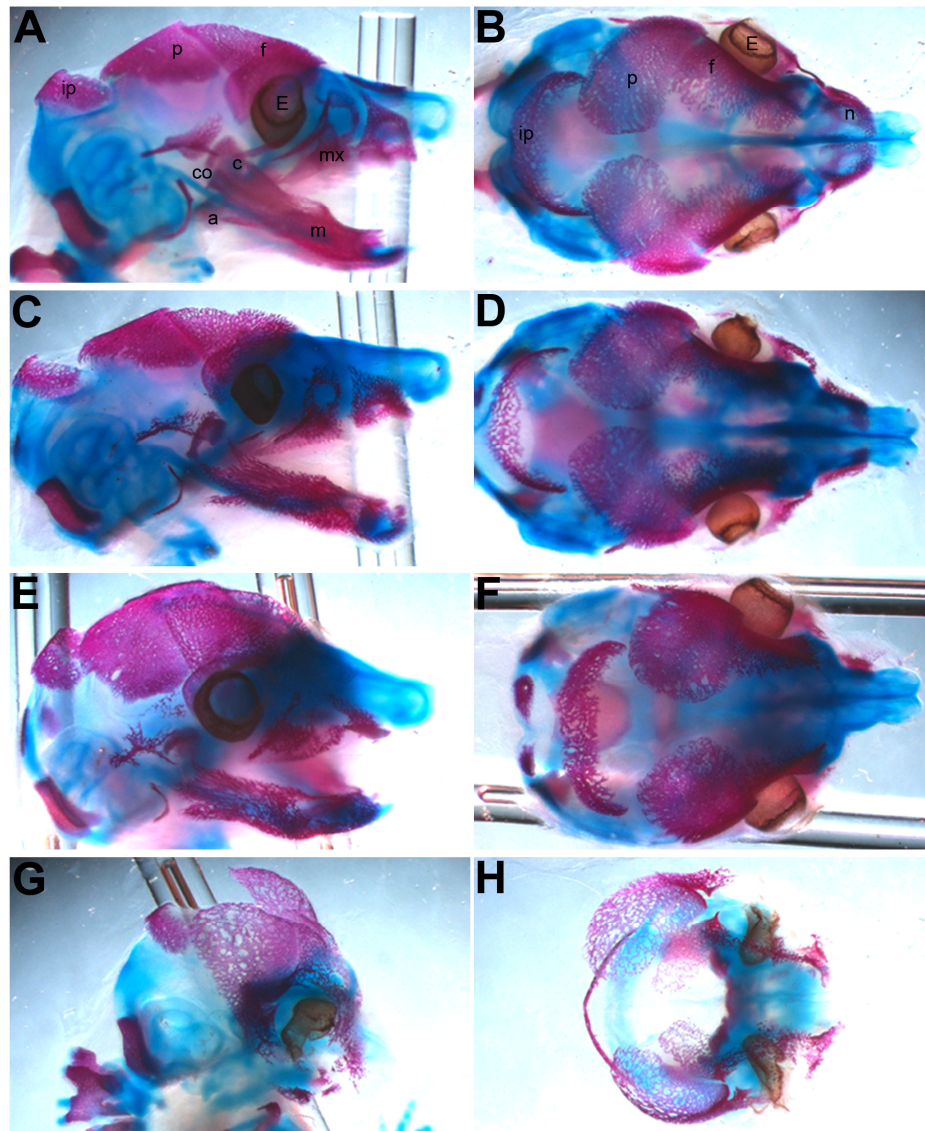


Figure 9. Defective cranial bone ossification in the *Bmp4* OE embryos.

Lateral (A,C,E,G) and top (B,D,F,H) view of E16.5 control (A-B) and *Bmp4* OE embryos (C-H) after skeletal analysis. *Bmp4* induction started at different time points: E13.5 (C-D), E12.5 (E-F), and E10.5 (G-H). a, angular process; c, coronoid process; co, condylar process; f, frontal bone; ip, interparietal bone; m, mandible; mx, maxillary; n, nasal bone; p, parietal bone.

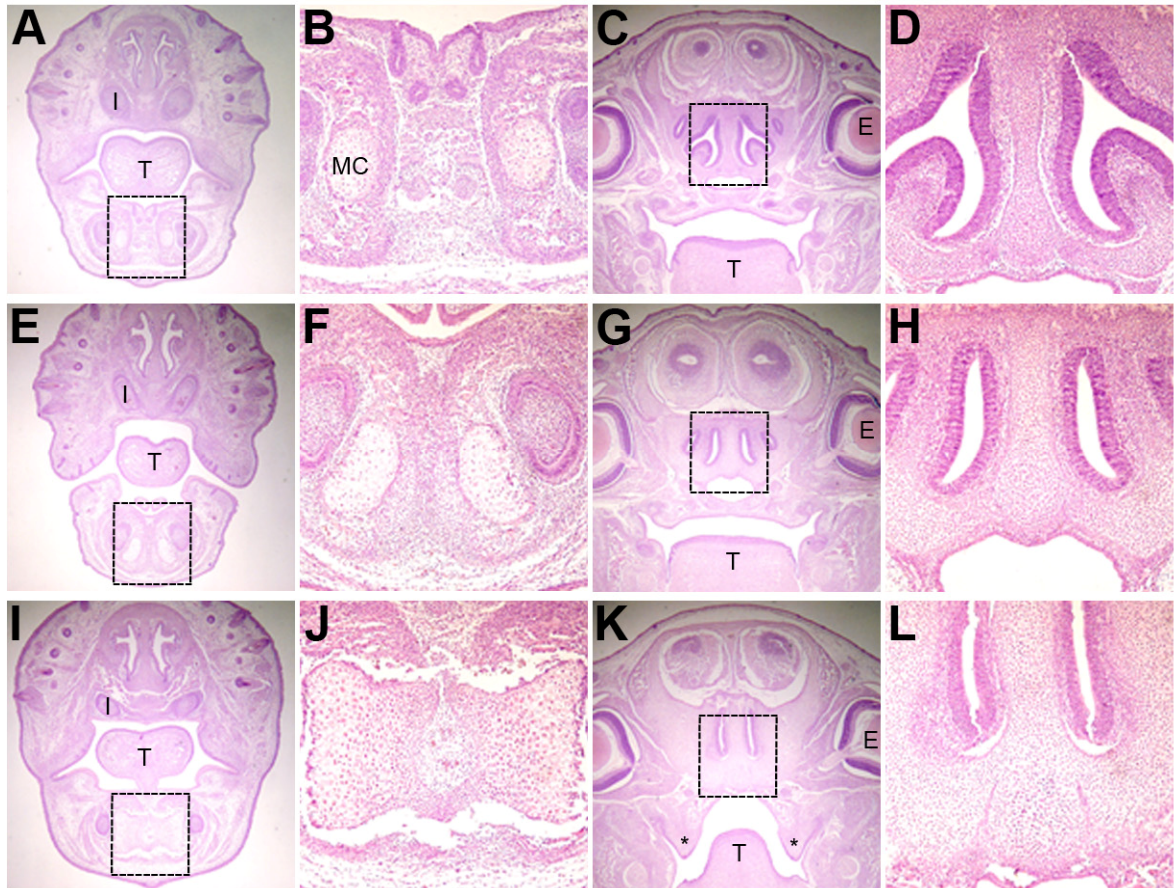


Figure 10. *Bmp4* OE embryos exhibit an expansion of the facial cartilage.

H&E staining of E16.5 control (A-D) and *Bmp4* OE embryos induced at E14.5 (E-H) and E12.5 (I-L). Meckel's cartilage is expanded in the *Bmp4* OE embryos. B, F and J are magnified view of dashed box in A, E and I, respectively. The nasal cartilage is also expanded in the *Bmp4* OE embryos. D, H and J are magnified view of dashed box in C, G and K, respectively. E, eye; I, incisor; MC, Meckel's cartilage; T, tongue. * indicate the cleft palate phenotype.

Histologic analysis indicated that *Bmp4* E12.5 induction resulted in a large increase in both nasal and Meckel's cartilage indicating that *Bmp4* modulates facial form by controlling both cartilage and bone development (Fig. 10 A-D, I-L). These *Bmp4* E12.5 induced embryos also had cleft palate (Fig. 10 K). Embryos induced at E14.5 show milder phenotypes indicating that *Bmp4* induced facial changes are stage dependent (Fig. 10 E-H). These findings indicate that increasing *Bmp4* levels regulated facial form in a stage-dependent fashion.

Expression profiling uncovers transcriptional regulators that are upregulated in the mandible of *Bmp4* gain of function embryos.

To comprehensively investigate genes regulated by Bmp-signaling in the mandibular process, we performed a microarray analysis. For this experiments, we used RNA extracted from mandibles of *Bmp4*OE and *Wnt1^{cre}; R26R^{rtTANagy}* control embryos that were induced with dox for 24 hours, starting at E10.5. Using a 2-fold change ($p < 0.05$) as threshold, we identified 144 down-regulated and 120 up-regulated genes (Fig. 11 A and Appendix 3). Gene ontology analysis for all genes revealed several gene clusters involved in various cellular processes, such as nucleic acid metabolism, cellular biosynthesis, regulation of gene expression and transcription activity (Fig. 11 B). Strikingly, among genes that were up-regulated after *Bmp4* induction, gene ontology indicated that transcriptional regulation was the main cellular process influenced by upregulated Bmp-signaling (Fig. 11 C and 12 A).

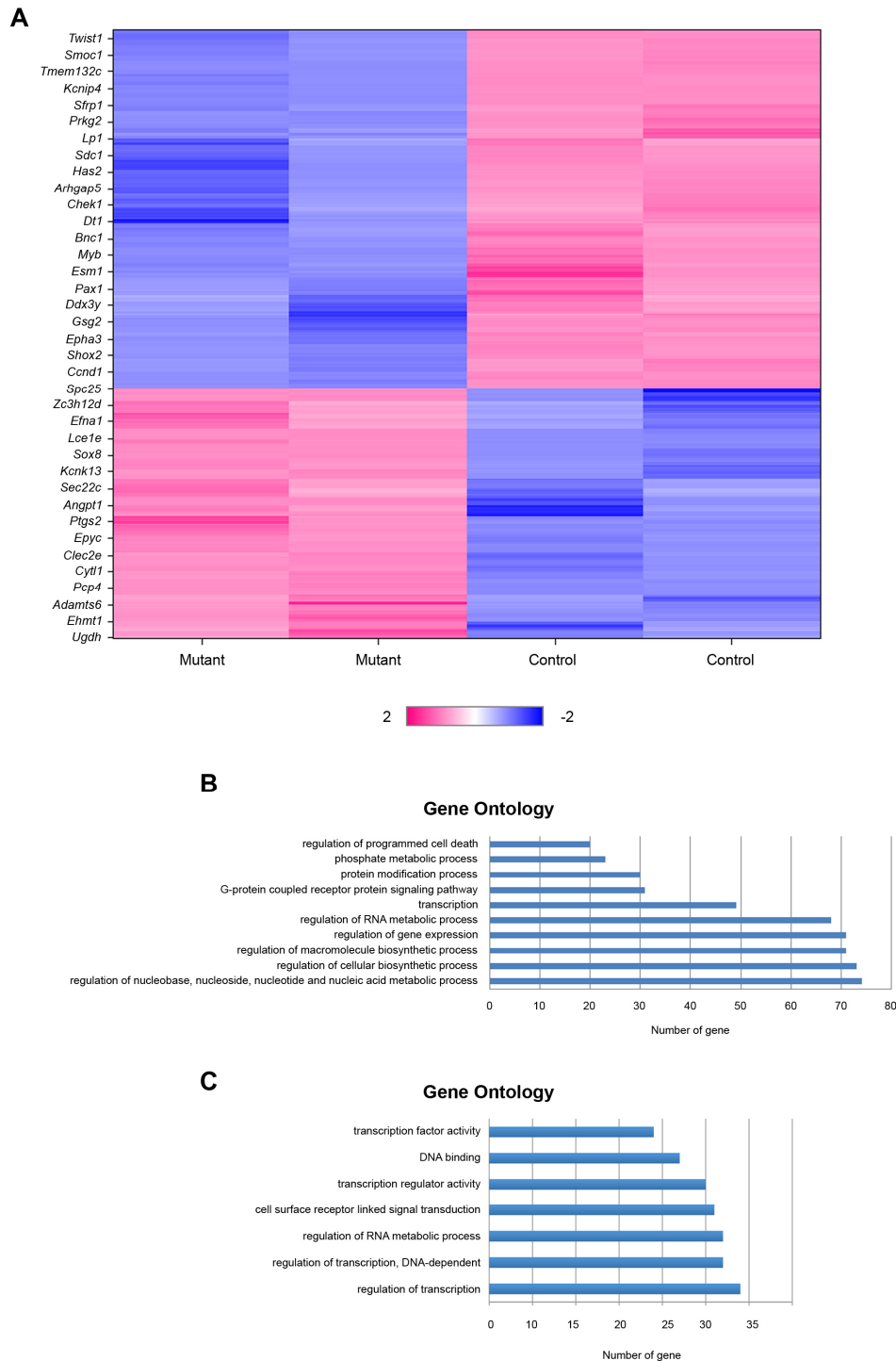


Figure 11. Differentially expressed genes in *Bmp4OE* mandibles.

(A) Heat map showing 264 genes that were differentially expressed (>2-fold) in the *Bmp4OE* mandibles; 120 were up-regulated (pink), while 144 were down-regulated (blue). (B) Gene Ontology analysis of 264 differentially expressed genes. (C) Gene Ontology analysis of up-regulated genes.

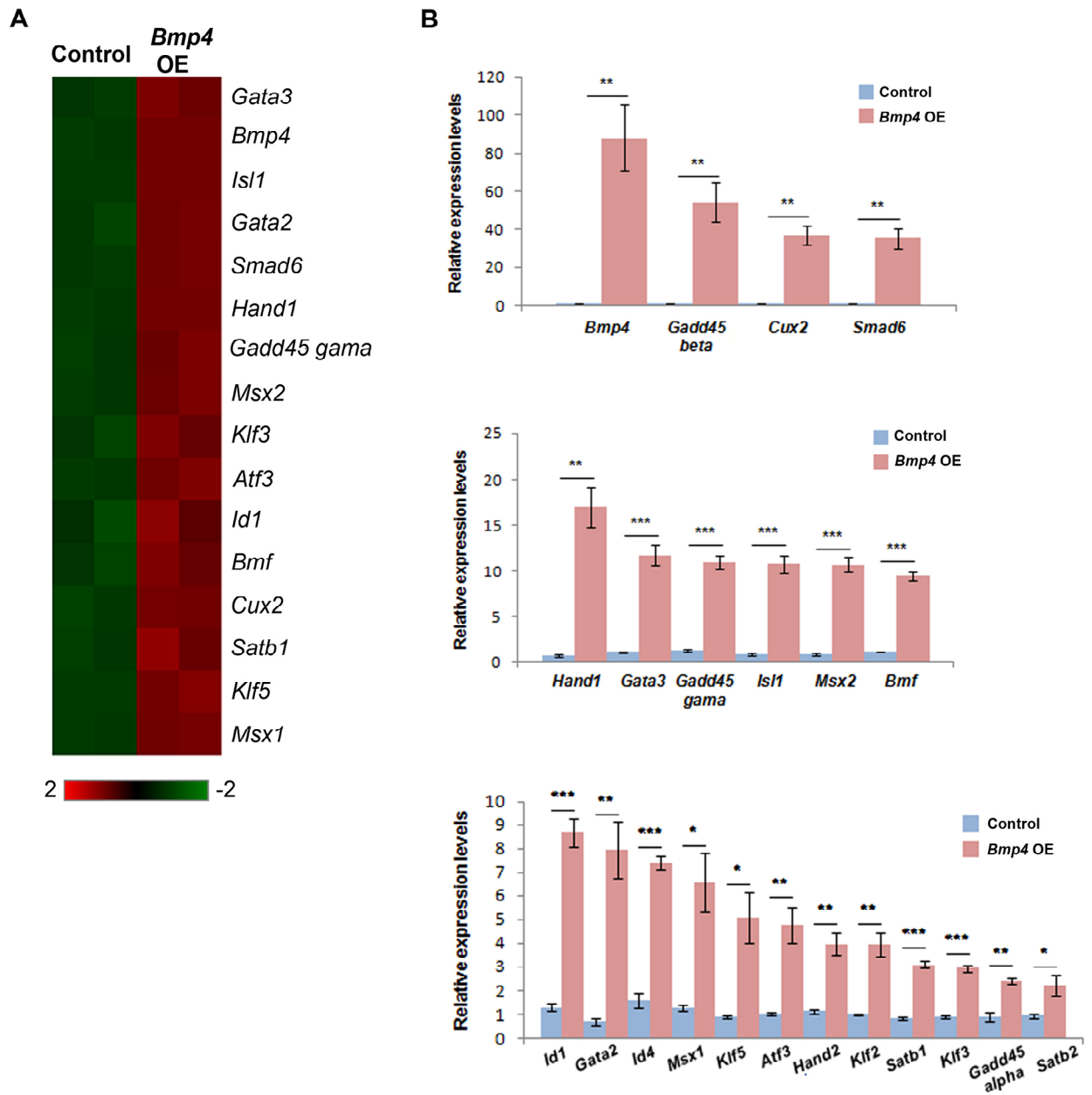


Figure 12. *Bmp4* gain of function in the neural crest cells leads to up-regulation of different transcriptional regulators.

(A) Heat map representing 16 transcriptional regulators that were upregulated in *Bmp4* OE mandibles (B) qRT-PCR validation of microarray results. Other genes from the same family were also included. * indicates a p-value < 0.05, ** indicates a p-value < 0.01, *** indicates a p-value < 0.001, error bars represent SEM.

In order to confirm the microarray results, we used independently generated RNA from control and *Bmp4* OE mandibles, and subjected them to qRT-PCR analysis. Included in the *Bmp4* induced genes (BIG) signature after qRT-PCR validation were multiple transcription factor families, including *Gata* genes, *Hand* genes, *Satb* genes and *Klf* genes (Fig. 12 B). Other upregulated transcriptional regulators include *Atf3*, *Cux2*, and *Isl1*. *Gata2*, *Hand2* and *Satb2* are transcription factors that play important roles in craniofacial development (Barbosa et al., 2007; Dobrev et al., 2006; Ruest et al., 2004b). Importantly, many of these genes (such as *Isl1* and *Id1*) have been shown to be targets of Smad-mediated signaling in other developmental processes and many have known roles in craniofacial development (Korchynskyi and ten Dijke, 2002; Mitsiadis et al., 2003). Interestingly, known negative regulators of Bmp-Smad signaling, *Gadd45* and *Smad6*, and *Noggin*, were also strongly upregulated in the *Bmp4* OE mandibles uncovering a negative feedback pathway in the mandible (Nohe et al., 2004; Suzuki et al., 2009).

We further validated the microarray experiments by *in situ* hybridization analysis of the RNA transcripts. *In situ* hybridization demonstrated an expanded expression pattern of the BIG signature after *Bmp4* induction (Fig. 13 and 14). Interestingly, there were distinct upregulated gene expression patterns. Some genes, such as *Hand1* and *Smad6* were broadly expanded throughout the CNC whereas other genes, such as *Gadd45 γ* and *Satb2*, were expanded in a more restricted region of the mandible (Fig. 13).



Figure 13. Expanded expression pattern of the BIG signature after *Bmp4* induction.

In situ hybridization on E11.5 embryos showing the change in the expression pattern of the indicated genes in the *Bmp4* OE.

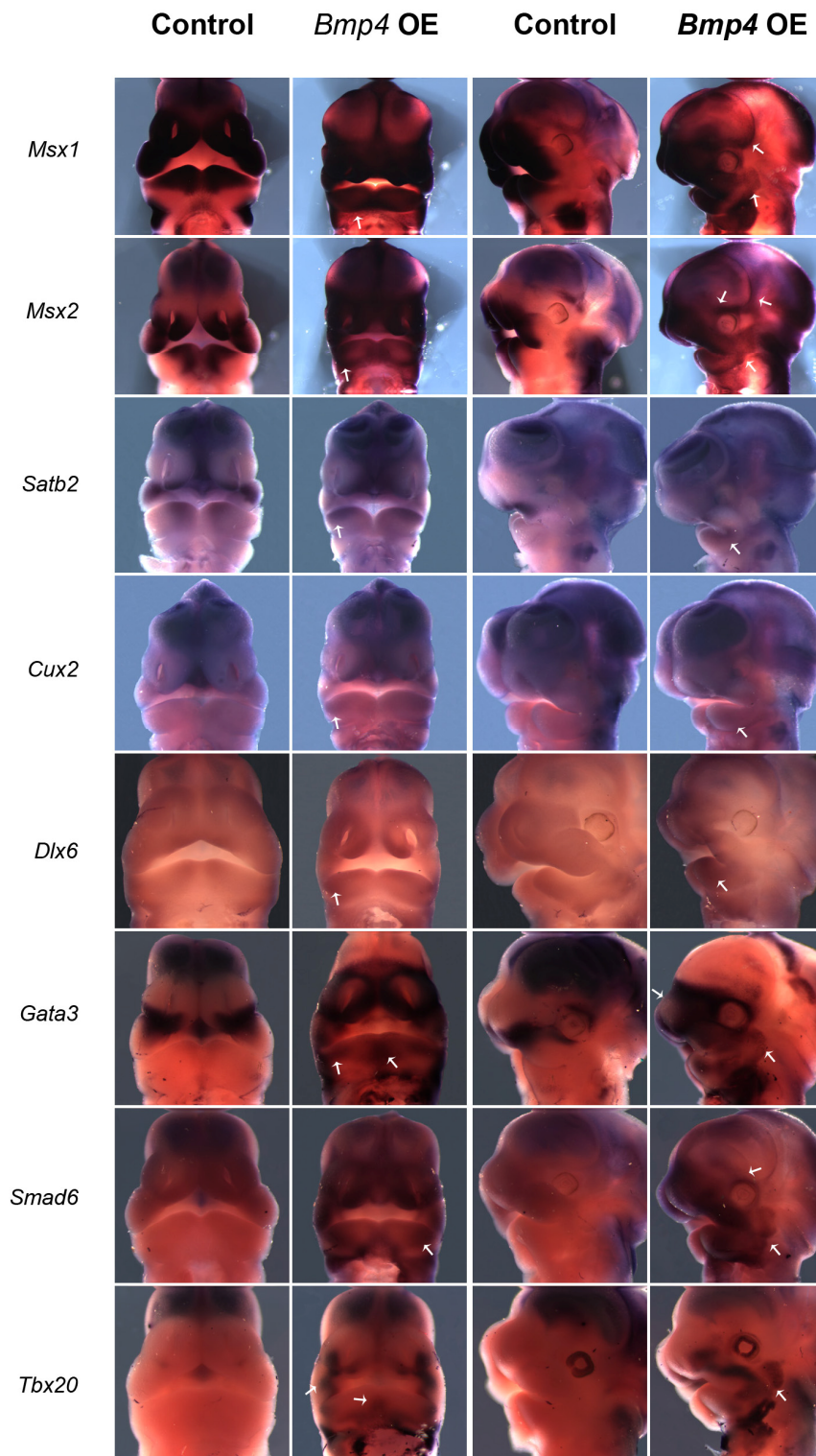


Figure 14. Expression patterns of up-regulated genes in *Bmp4*OE embryos.

In situ hybridization on E11.5 controls and *Bmp4*OE embryos, showing the change in the expression pattern of the indicated genes.

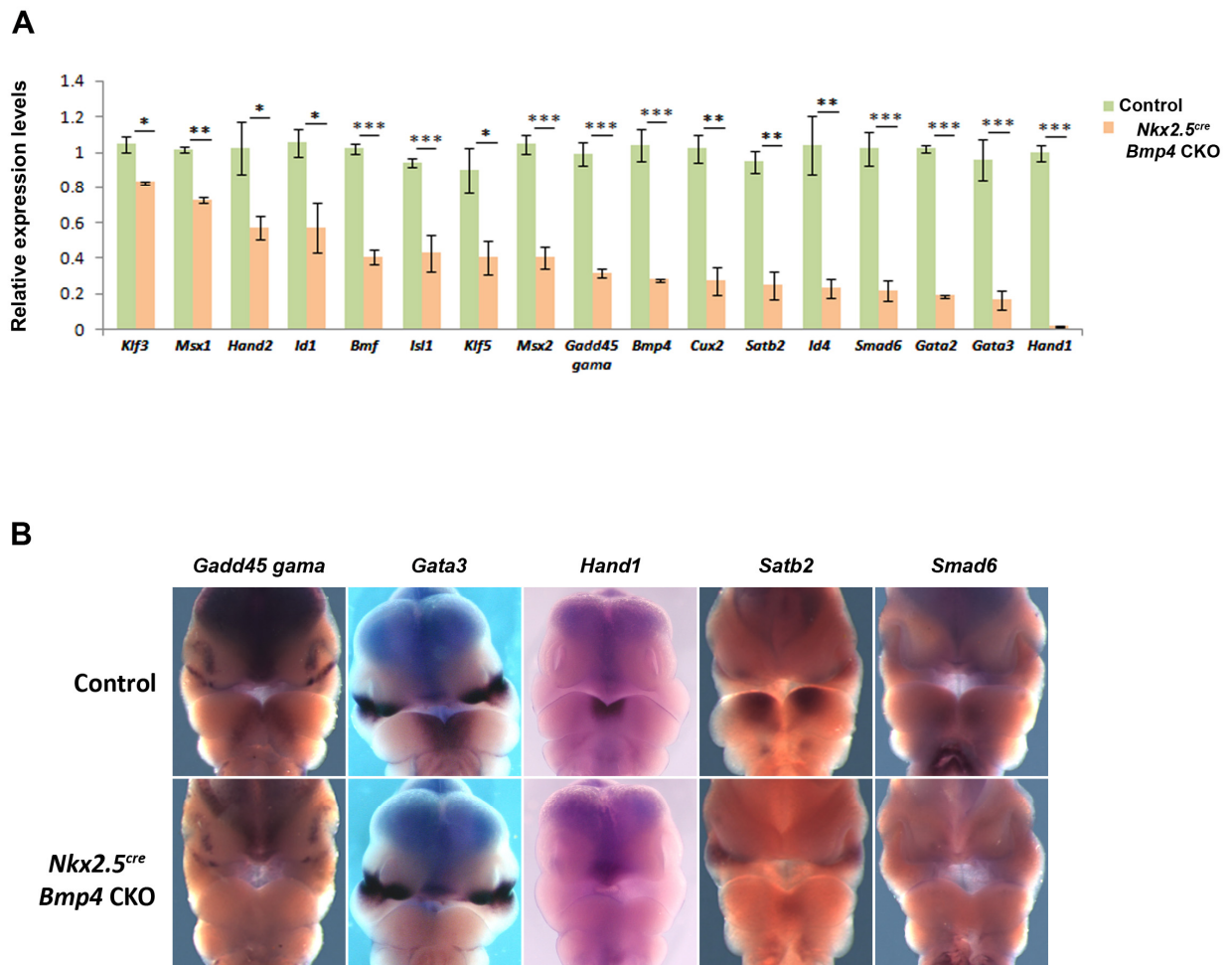


Figure 15. Bmp deficiency results in reduced mandibular expression of Bmp-regulated genes. (A) qRT-PCR of E11.5 control and *Nkx2.5^{cre}*; *Bmp4* CKO mandibles. (B) *In situ* hybridization on E11.5 embryos showing the change in the expression pattern of the indicated genes in the *Nkx2.5^{cre}*; *Bmp4* CKO. * indicates a p-value < 0.05, ** indicates a p-value < 0.01, *** indicates a p-value < 0.001, error bars represent SEM.

Common target genes that are expanded in the *Bmp4* OE embryos are also downregulated in *Bmp* loss of function embryos.

To determine whether the same sets of genes that are upregulated in the *Bmp4* OE embryos were also reduced in the *Bmp* loss of function embryos, we evaluated the expression of the candidate genes in response to decreased Bmp-Smad activity. Because the *Wnt1^{cre}; Bmp2/4/7* triple mutants are recovered at low frequencies, we supplemented our experiments with the *Nkx2.5^{cre}; Bmp4^{n/f}* embryos that have greatly reduced Bmp-signaling in the mandibular ectoderm and mesenchyme (Liu et al., 2005a). qRT-PCR analysis of the mandibular tissue showed significant reduction in the expression levels of genes that were up-regulated in the *Bmp4* OE tissue (Fig. 15 A). Moreover, whole mount *in situ* analysis for a subset of these genes revealed loss of mandibular expression in *Bmp4* mutant embryos (Fig. 15 B).

Subsets of transcriptional regulators are direct *Bmp4* targets.

The up-regulation of *Gadd45γ*, *Gata3*, *Hand1*, *Satb2* and *Smad6* transcripts in a cell environment rich in *Bmp4* signaling, as well as, their down-regulation in the absence of *Bmp4* (Fig. 13 and Fig. 15 B), give rise to the possibility that these genes are direct targets of *Bmp4* signaling. To determine whether these BIG signature genes were directly regulated by Smad-mediated transcription, we undertook a bioinformatic approach to identify conserved Smad recognition elements within a 5Kb region located in the 5' flanking region of these genes. For

Gadd45γ, *Gata3*, *Hand1*, *Satb2* and *Smad6*, we uncovered phylogenetically conserved Smad recognition elements (Fig. 16 A). We tested the ability of Smad1/5 to bind to these sequences *in vivo* by ChIP assays in wild-type mandibles and in the mouse osteoblastic *cell* line, *MC3T3*-E1. Our data indicate that in the developing mandible, Smad1/5 binds directly to the chromatin of these five genes (Fig. 16 B). Moreover, in *MC3T3*-E1 cells that were cultured in the presence of Bmp4, we found an increased enrichment in Smad1/5 chromatin binding after Bmp treatment (Fig. 16 C).

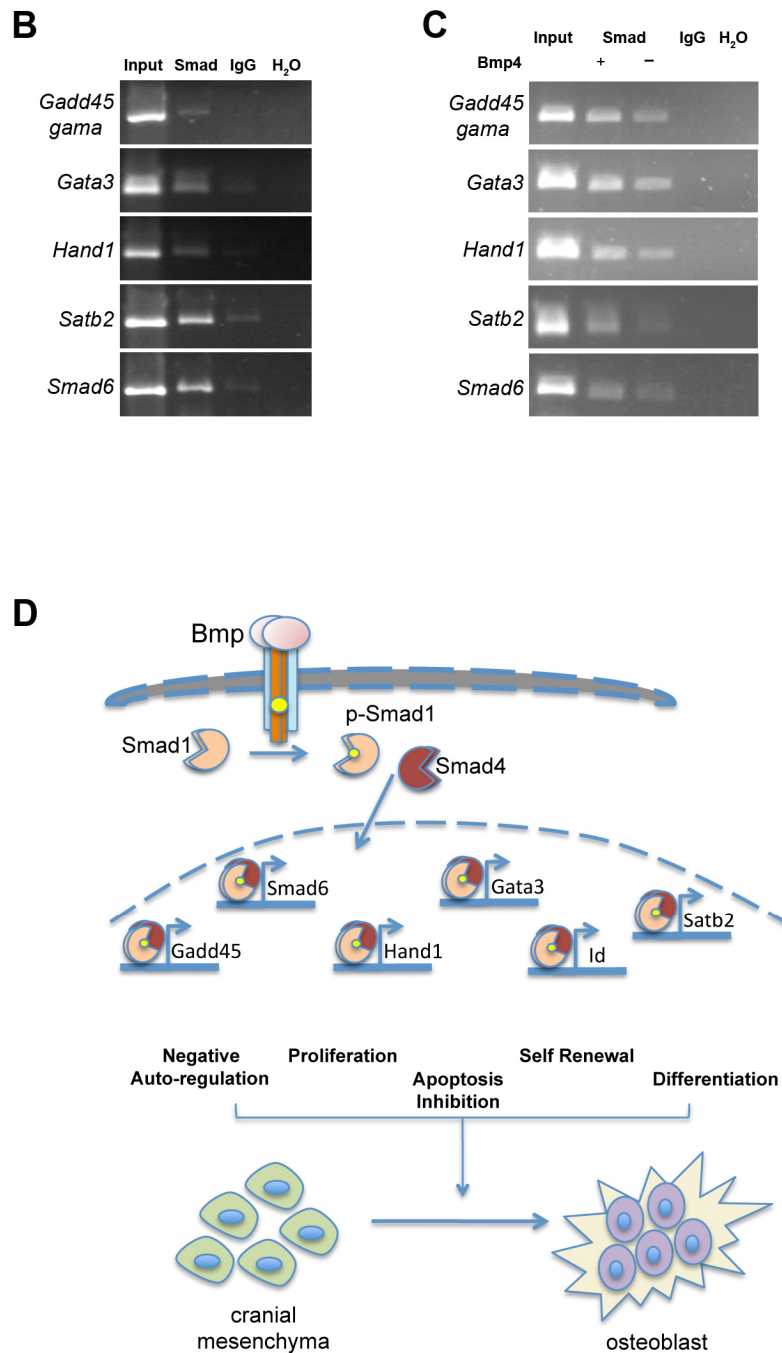


Figure 16. Direct, Smad-mediated regulation of a subset of Bmp-induced genes.

(A) Sequence alignment showing the conservation among species of the putative Smad1 binding site. ChIP assay using (B) E11.5 wild-type mandibles and (C) MC3T3-E1 cells culture for 12 hrs in the absent or presence of 25pg/ul of Bmp4. (D) Bmp regulates craniofacial skeletal development by balancing self-renewal and differentiation in the CNC progenitors

Discussion

We performed a comprehensive analysis of Bmp function in CNC using genetics, gene expression profiling, and ChIP. Our profiling and qRT-PCR validation data from the *Bmp4* OE embryos indicate that the BIG signature contains twenty-one genes. Moreover, we validated seventeen of the twenty-one genes in the Bmp loss of function model revealing that Bmp is necessary and sufficient for expression of those seventeen genes.

Our data reveal that Bmp controls bone morphogenesis and facial form *via* common target genes. The BIG signature was upregulated in *Bmp4* OE embryos with facial form changes and reduced in Bmp deficient embryos with severe bone morphogenesis phenotypes. Within the BIG signature are transcriptional regulators important for osteoblast differentiation and progenitor cell self-renewal. Bmp-signaling also induces a negative regulatory pathway that likely functions as a buffering mechanism to maintain precise Bmp-signaling levels. We show that six genes, *Gata3*, *Gadd45γ*, *Hand1*, *Satb2*, and *Smad6*, are directly bound by Smad 1/5. Our findings indicate that a balance between self-renewal and progenitor differentiation in CNC underlies Bmp-regulated facial form control and bone morphogenesis (Figure 16 D).

Direct Bmp target genes regulate cranial neural crest progenitor self-renewal.

Our data show that Bmp-signaling in CNC progenitors regulates genes that are directly implicated in self-renewal such as Id and Klf genes. *Klf2* and *Klf5*, as

well as *Id1* and *Id4* are regulated by Bmp-signaling in CNC progenitors. Klf genes, regulators of ES cell self-renewal by controlling *Nanog* expression and cellular reprogramming, have not been shown to be regulated by Bmp-signaling (Zhang et al., 2010). Our findings suggest that Bmp-signaling in CNC promotes limited self-renewal of CNC cells that allow progenitor cells to persist for a short time as craniofacial development progresses.

In other *in vivo* model systems, such as the *Drosophila* ovary, Bmp signaling promotes self-renewal and proliferation of somatic stem cells and prolongs progenitor lifespan (Kirilly et al., 2005). In CNC progenitors, it is conceivable that Bmp-signaling increases the number of self-renewing progenitor cells in addition to activating expression of the CNC self-renewal program.

In addition to inducing *Id1* expression in embryonic stem cells, Bmp-signaling directly promotes self-renewal in collaboration with leukemia inhibitory factor through a direct interaction between Smad1 and the core self-renewal factors Nanog, Oct4 and Sox2 (Chen et al., 2008; Fei et al., 2010; Ying et al., 2003). As defined by ChIP seq, Smad1 commonly occupies Nanog-Oct4-Sox2 bound loci revealing that Bmp-signaling directly interacts with the core pluripotency machinery to enhance pluripotency and self-renewal. Moreover, the Smad1-containing complexes in ES cells recruit the HAT p300 to activate gene transcription (Chen et al., 2008). Our findings support a model in which Bmp-signaling enhances CNC progenitor self-renewal by activating the self-renewal gene program. Future ChIP seq experiments will be required to determine if Smad1 directly interacts with a pluripotency program in CNC progenitors.

Bmp promotes osteoblast differentiation from CNC progenitors.

Bmp-signaling also regulates lineage-restricted genes such as *Satb2* that enhance osteoblast lineage development. *Satb2* is a DNA binding and architectural factor that has a positive role in osteoblast development. *Satb2* deficiency results in phenotypes that are similar to mild Bmp loss of function phenotypes such as cleft palate and calvarial defects with shortened mandible. Importantly, *Satb2* controls osteoblast differentiation through regulation of *Runx2* and *Atf4* expression (Dobrev et al., 2006). Notably, similar to *Bmp4*, *Satb2* deficiency causes orofacial clefting in humans as well as mice (Britanova et al., 2006). Our data shows that *Satb2* is a direct Smad1/5 target indicating that a major pathway for Bmp-regulated bone development and facial form regulation is through *Satb2* function.

Similar to *Bmp4* loss of function mutants, *Gata3* mutants have a medial mandibular deficiency (Liu et al., 2005a; Ruest et al., 2004a). There is evidence that *Gata3* directly regulates *N-myc* in the branchial arches suggesting that one cellular mechanism in the *Gata3* mutant mandible is reduced proliferation (Potvin et al., 2010). Other data also indicate that *Gata3* promotes osteoblast and neuron survival suggesting that in addition to proliferation, apoptosis may also be enhanced in *Gata3* mutants as it is in *Bmp4* loss of function embryos (Chen et al., 2010; Liu et al., 2005a; Tsarovina et al., 2010).

Hand1 and *Hand2* have overlapping function in medial mandible development, and promote progenitor cell proliferation and inhibit differentiation (Barbosa et al., 2007; Funato et al., 2009). In the heart, *Hand1* overexpression

increases cell proliferation indicating that the Hand mandibular defect may result from reduced progenitor cell proliferation. It is interesting to note that both *Hand1* and *Gata3* have been implicated in trophoblast development indicating that these two genes may have interrelated functions in multiple cellular contexts (Ralston et al., 2010).

In addition to Bmp-signaling, the Endothelin (Edn) signaling pathway regulates *Hand* gene expression and also is critically important in facial form regulation. *Edn* deficient embryos display mandibular to maxillary transformations that are restricted to the Hox negative CNC (Gitton et al., 2010). Moreover, gain of function experiments indicate that expanded *Edn* and *Hand2* in maxillary process results in transformation to a mandibular phenotype. Our data indicate that Bmp and Edn-signaling converge on Hand gene function to regulate facial form.

The *Dlx 5/6* genes, targets for Edn-signaling and direct regulators of *Hand2*, are also critically important in facial form development (Depew et al., 2002). Only modest *Dlx6* expansion in *Bmp4* OE embryos indicate that Bmp induced regulation of Hand genes primarily goes directly through Smad 1/5 (Fig. 14).

Bmp-regulated negative feedback loops are critical for mandible development

Negative auto-regulation is a mechanism to confer robustness to the developing embryo by buffering the system from elevated Bmp levels and is critical for normal craniofacial and heart development (Paulsen et al., 2011; Prall et al., 2007). *Bmp4* induced expression of genes that are negative regulators of Bmp-

signaling such as *Smad6*, *Noggin*, and *Gadd45*. The importance of finely tuned Bmp-signaling levels in mice and humans is apparent from *Noggin* loss of function studies in mice as well as human genetics studies. *Noggin* deficiency results in cleft palate, defective mandibular development, as well as limb and heart defects (Brunet et al., 1998; Choi et al., 2007; Gong et al., 1999; He et al., 2010). The negative auto-regulatory pathway includes two genes, *Gadd45 γ* and *Smad6* that are Smad-regulated direct Bmp targets. Moreover, the negative auto-regulatory pathway modulates the pathway by multiple mechanisms. *Smad6* inhibits R-Smad activity by both competing for Smad4 and also inhibiting R-Smad phosphorylation. *Gadd45 γ* promotes ubiquitin ligase interaction with the Smad linker region to destabilize R-Smad, while *Noggin* is a competitive inhibitor of the Bmp ligand-receptor interaction (Sheng et al., 2010).

Bmp-signaling controls expression of multiple families of transcriptional regulators

Cux2 has not been previously connected to Bmp-signaling or bone morphogenesis. The closely related gene, *Cux1*, is regulated by Tgf- β and represses collagen expression. *Cux2* is regulated by Notch in the spinal cord where it controls cell cycle progression and promotes interneuron fate. *Cux2* also has been shown to regulate dendrite morphology in post-natal brain (Iulianella et al., 2009; Iulianella et al., 2003).

Among the other Bmp-regulated genes that we identified, are genes that were previously shown to be Bmp-regulated. Previous experiments uncovered a Bmp-Msx genetic pathway in multiple contexts within the developing craniofacial apparatus including skull, palate and teeth (Chai and Maxson, 2006). Our data also indicate that *Is/1* is regulated by Bmp-signaling during mandibular development. There is evidence that Bmp and *Is/1* function in a positive feedback loop in the mandible (Mitsiadis et al., 2003). Our data support these earlier findings and substantially extend previous understanding of Bmp targets in craniofacial development.

Future direction

Our *in situ* data indicate that in the *Bmp4* OE embryos one gene group including *Gata3*, *Hand1*, and *Smad6* was broadly expressed throughout the cranial neural crest in response to *Bmp4* overexpression. In contrast, genes such as *Satb2* and *Gadd45 γ* were more resistant to *Bmp4* overexpression and were upregulated in a more discrete spatial pattern. This observation exposes the possibility of other regulatory mechanisms capable of fine-tune the expression of *Satb2* and *Gadd45 γ* .

miRNA are small non-coding RNAs that post transcriptionally regulate gene expression by enhancing mRNA degradation or by inhibiting translation (Bartel, 2009). Recently studies show the participation of Bmp induced Smad signaling activity during the transcription of microRNA (miRNA). It has been revealed capability of Smad1/5 to directly bind to the Drosha complex to promote microRNA

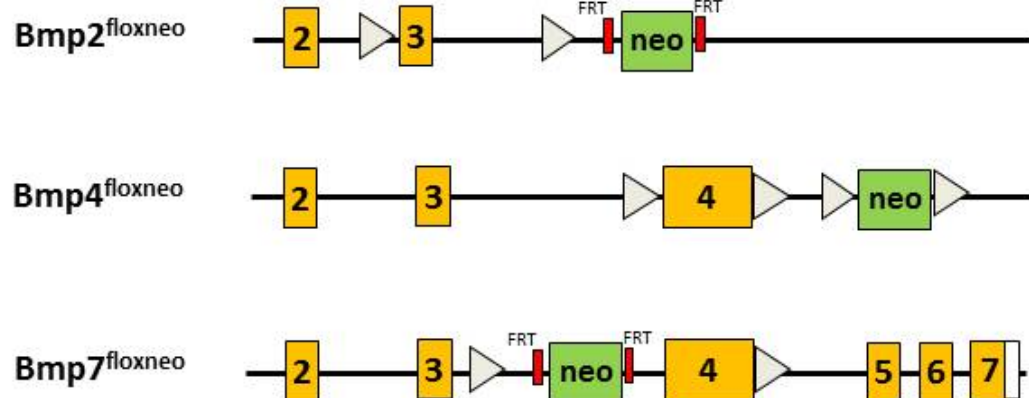
(miR) processing (Davis et al., 2008). Furthermore, our group has shown that Bmp-signaling can induce miR transcription through a canonical Smad regulated mechanism (Wang et al., 2010).

To test the possibility of miRNA involvement in the *Bmp4* OE embryos phenotypes, we can simultaneously induce heterozygosity of *Dicer* in the *Bmp4* OE embryos (*Wnt1cre*; *Bmp4*^{teto}; *R26Nagy*^{+/-}; *Dicer*^{f/+}). If the elevated levels of *Bmp4* observed in the *Bmp4* OE embryos are triggering a miRNA activation pathway, heterozygosity of *Dicer* should suppress some of the phenotype observed in the *Bmp4* OE embryos.

One idea is that other signaling pathways, such as Wnts, may regulate miR expression that then degrades target mRNAs in certain domains of the branchial arches. Alternatively, the distinct responses to Bmp4 signaling may be regulated at the level of chromatin regulation such that Smad mediated activation is offset by negative regulatory mechanisms that cannot be overcome by high levels of Bmp-signaling.

Appendix

Appendix 1. *Bmp2*, *Bmp4*, and *Bmp7* conditional null alleles.



Appendix 2. Primers sequence for qRT-PCR and ChIP experiments.

	Forward Primer	Reverse Primer
qRT-PCR		
<i>Atf3</i>	5'- CTG CTG CCA AGT GTC GAA ACA -3'	5'- TCA GCT CAG CAT TCA CAC TCT -3'
<i>Bmf</i>	5'- TAT TGC AGA CCA GTT CCA TCG -3'	5'- TCT TGT CTG TTC AGG GCG AGG -3'
<i>Bmp4</i>	5'- AGG AAG AGC AGA GCC AGG GAA -3'	5'- TGC TGC TGA GGT TGA AGA GGA -3'
<i>Cux2</i>	5'- TGA CAC CCG AGC AGT ATG AAC -3'	5'- AGA TGC CGT TCT TGG CTA GCT -3'
<i>Ehmt1</i>	5'- AAC ACA AGA GCT AGC CCA CAG -3'	5'- TGA AGT CGT CAG CTG TGA CAT -3'
<i>Gadd45 alpha</i>	5'-AGC AGA AGA CCG AAA GGA TGG ACA-3'	5'-AGC AGG CAC AGT ACC ACG TTA T-3'
<i>Gadd 45 beta</i>	5'-TAC GAG GCG GCC AAA CTG ATG AAT-3'	5'-ACG ACT GGA TCA GGG TGA AGT GAA-3'
<i>Gadd 45 gama</i>	5'-ATG TGG ACC CTG ACA ATG TGA CCT-3'	5'-GCA GAA CGC CTG AAT CAA CGT GAA-3'
<i>Gapdh</i>	5'- TGG CAA AGT GGA GAT TGT TGC -3'	5'- AAG ATG GTG ATG GGC TTC CCG -3'
<i>Gata2</i>	5'- TTG TCA GAC GAC AAC CAC CAC -3'	5'- TTC CTT CTT CAT GGT CAG TGG -3'
<i>Gata3</i>	5'- ACT CCA GTC CTC ATC TCT TCA -3'	5'- TGC ACC TGA TAC TTG AGG CAC -3'
<i>Hand1</i>	5'- AGA GGA GAC GCA CAG AGA GCA -3'	5'- TTG ATC TTG GAG AGC TTG GTG -3'
<i>Hoxa2</i>	5'- GTG GTT TCA GAA CCG GAG AA -3'	5'- GGG CTT GCT CAA AGA GTG AC -3'
<i>Id1</i>	5'- AAC GTC CTG CTC TAC GAC ATG -3'	5'- TTA CAT GCT GCA GGA TCT CCA -3'
<i>Id4</i>	5'- GCA GTG CGA TAT GAA CGA CTG -3'	5'- TAA CGT GCT GCA GGA TCT CCA -3'
<i>Klf2</i>	5'- CTA AAG GCG CAT CTG CGT A -3'	5'- TAG TGG CGG GTA AGC TCG T -3'
<i>Klf3</i>	5'- TGC AAG AGA ACC ATC CTT CCG -3'	5'- TGC ACC CAT CAT AGT CGC ATC -3'
<i>Klf4</i>	5'- CGG GAA GGG AGA AGA CAC T -3'	5'- GAG TTC CTC ACG CCA ACG -3'
<i>Klf5</i>	5'- AGT TCG ACA AAC CAG ACG GCA -3'	5'- GGC ATG CCC TGG AAC TGT TTC -3'
<i>Satb1</i>	5'- AGT GCC CCC TTT CAC AGA G -3'	5'- TGC TGC TGA GAC ATT TGC AT -3'
<i>Satb2</i>	5'- AAC CAA CAG ATA GCC GTT AGC -3'	5'- TCC ACA GAG GAG TTT GTT GGC -3'
<i>Smad6</i>	5'- TGA CCT GCT GTC TCT TCT CCG -3'	5'- TTG AGC CTC TTG AGC AGC GAG -3'
ChIP		
<i>Gadd45g</i>	5'-AGTGAGCTGTACACCAAGGCT-3'	5'-ACAAACGGATTCTTGGTCCTG-3'.
<i>Gata3</i>	5'-TCTCCCTGGGTTCTCGCCA-3'	5'-TCACTTCCCATTCCAGCTCGA-3'
<i>Hand1</i>	5'-AACCCGCAGGGCACAAGAA-3'	5'-TGTTGTGCAAGAGATTGTGA-3'
<i>Satb2</i>	5'-GCGCGTTTCCCGAAACCGAAT-3'	5'-AAATATGAACAGTCCTCTCC-3'
<i>Smad6</i>	5'-GCGCGAGCTCCCTCATGTT-3'	5'-ACCTGAACATACGATACCCTT-5'

Appendix 3. List of statistically significant genes that were differentially expressed in the mandible after *Bmp4* over-expression.

probe id	<i>Bmp4</i> OE vs Control (FoldChange)	<i>Bmp4</i> OE vs Control (Pvalue)	Ensembl Gene Symbol	Ensembl Gene Description
mMC004687	-13.1	0.0004	Cbln4	Cerebellin-4 precursor.
mMC004895	-12.75	0.0021	Osr2	Protein odd-skipped-related 2.
mMC007461	-8.88	0.0002	Barx1	Homeobox protein BarH-like 1.
mMC001824	-7.55	0.0017	Shox2	Short stature homeobox protein 2.
mMC006410	-7.53	0.0026	Smoc1	SPARC-related modular calcium-binding protein 1 precursor
mMC011279	-7.26	0.0023	Smoc2	SPARC-related modular calcium-binding protein 2 precursor
mMC013934	-7.25	0.0032	Meox2	Homeobox protein MOX-2.
mMR028474	-6.55	0.0029	Cyp1b1	Cytochrome P450 1B1.
mMC018294	-6.15	0.0016	Bnc1	Zinc finger protein basonuclin-1.
mMR028929	-5.25	0.0017	Tbx15	T-box transcription factor TBX15.
mMC001020	-5.1	0.0093	Osr1	Protein odd-skipped-related 1.
mMC002854	-4.87	0.0004	Cr1f1	Cytokine receptor-like factor 1 precursor.
mMC023938	-4.72	0.0132	Pax1	Paired box protein Pax-1.
mMC005050	-4.66	0.0006	Prr6	Proline-rich protein 6.
mMC004704	-4.42	0.0031	Wnt2	Protein Wnt-2 precursor.
mMC017469	-4.26	0.0035	Dkk4	Dickkopf-related protein 4 precursor.
mMC024318	-4.23	0.0004	Angptl1	Angiopoietin-related protein 1 precursor.
mMC001087	-4.18	0.006	Has2	Hyaluronan synthase 2.
mMC006133	-4.08	0.0041	Aldh1a2	Retinal dehydrogenase 2.
mMC012585	-4.08	0.0026	Cyp26a1	Cytochrome P450 26A1.
mMC023854	-4	0.026	Eya4	Eyes absent homolog 4.
mMC011362	-3.95	0.0004	Sfrp2	Secreted frizzled-related protein 2 precursor.
mMR028699	-3.89	0.0152	Birc5	Baculoviral IAP repeat-containing protein 5.
mMC020668	-3.78	0.0002	Tgfr3	TGF-beta receptor type III precursor.
mMC010520	-3.75	0.0011	Prdx2	Peroxiredoxin-2.
mMC006582	-3.73	0.0013	Thy1	Thy-1 membrane glycoprotein precursor.
mMR026812	-3.61	0.0178	Cdk5r1	Cyclin-dependent kinase 5 activator 1 precursor.
mMC011387	-3.6	0.0009	Tbc1d2	TBC1 domain family, member 2.
mMC004686	-3.57	0.0017	Irx2	Iroquois-class homeodomain protein IRX-2.
mMR027206	-3.44	0.0008	Spp1	Osteopontin precursor (Bone sialoprotein 1)
mMC014693	-3.32	0.0079	Bnc2	Zinc finger protein basonuclin-2.
mMC012271	-3.27	0.0028	Col8a1	Collagen alpha-1(VIII) chain precursor.
mMC015778	-3.12	0.0075	Mkx	Homeobox protein Mohawk.
mMC009536	-3.09	0.0041	Adora2b	Adenosine receptor A2b.
mMC009633	-3.07	0.0065	Pax3	Paired box protein Pax-3.
mMC007876	-3.06	0.0029	Ddit4l	DNA-damage-inducible transcript 4-like protein.
mMC005287	-3.01	0.0032	Etv5	ETS translocation variant 5.
mMC020953	-3	0.0048	Sfrp1	Secreted frizzled-related protein 1 precursor (sFRP-1).
mMC004112	-3	0.0043	Mmd2	Monocyte to macrophage differentiation factor 2.
mMC011604	-2.99	0.0068	Twist2	Twist-related protein 2 (Dermo-1).
mMC012120	-2.99	0.0003	Ccne1	G1/S-specific cyclin-E1.
mMC016088	-2.92	0.0044	Hey2	Hairy and enhancer of split-related protein 2.
mMC016113	-2.88	0.0048	Emx2	Homeobox protein EMX2 (Empty spiracles homolog 2).
mMC024238	-2.87	0.0006	Hoxd8	Homeobox protein Hox-D8 (Hox-4.3) (Hox-5.4).
mMC011610	-2.87	9.35E-05	Lingo2	leucine rich repeat and Ig domain containing 2.
mMC019146	-2.84	0.0079	Tnc	Tenascin precursor (TN) (Tenascin-C).

mMR027081	-2.84	0.0011	Jarid1d	Histone demethylase JARID1D.
-----------	-------	--------	---------	------------------------------

probe id	Bmp4 OE vs Control (FoldChange)	Bmp4 OE vs Control (Pvalue)	Ensembl Gene Symbol	Ensembl Gene Description
mMC005059	-2.81	0.0046	Kif4	Chromosome-associated kinesin KIF4 (Chromokinesin).
mMC014576	-2.78	0.0043	Agtr1a	Type-1A angiotensin II receptor (AT1) (AT1A).
mMC011224	-2.76	0.0003	Lhx8	LIM/homeobox protein Lhx8.
mMC016964	-2.76	0.0005	Mxd3	Max-interacting transcriptional repressor MAD3.
mMR029106	-2.76	1.90E-05	Tbx18	T-box transcription factor TBX18 (T-box protein 18).
mMC025853	-2.75	0.0072	Col23a1	Collagen alpha-1(XXIII) chain.
mMC007337	-2.72	0.0151	Acadm	Medium-chain specific acyl-CoA dehydrogenase.
mMC006073	-2.63	0.0047	Nt5e	5'-nucleotidase precursor.
mMR027782	-2.63	0.0014	Tcfap2c	Transcription factor AP-2 gamma (AP2-gamma).
mMC007882	-2.6	0.0025	Phf17	Protein Jade-1 (PHD finger protein 17).
mMC013088	-2.58	0.0091	Calca	Calcitonin gene-related peptide 1 precursor.
mMC021257	-2.57	0.0104	Bub1	Mitotic checkpoint serine/threonine-protein kinase BUB1 .
mMR027630	-2.56	0.0019	Ccnd1	G1/S-specific cyclin-D1.
mMR027330	-2.55	0.0194	Fgf10	Fibroblast growth factor 10 precursor.
mMC023785	-2.54	0.0083	Lhx9	LIM/homeobox protein Lhx9.
mMC015557	-2.53	0.0007	Col27a1	Collagen alpha-1(XXVII) chain precursor.
mMC011218	-2.52	0.0004	Fanci	Fanconi anemia group I protein homolog.
mMC005685	-2.51	0.0019	Dlx1	Homeobox protein DLX-1.
mMC004336	-2.51	0.0115	Recql4	ATP-dependent DNA helicase Q4.
mMC020644	-2.5	0.0131	Bok	Bcl-2-related ovarian killer protein (Matador protein).
mMC002917	-2.5	0.0033	Epha3	Ephrin type-A receptor 3 precursor.
mMR029325	-2.48	0.0016	Col6a3	Collagen alpha3(VI) precursor (Fragment).
mMC024692	-2.47	0.0031	Ccnd1	G1/S-specific cyclin-D1.
mMR030518	-2.46	0.002	Ddx3y	ATP-dependent RNA helicase DDX3Y.
mMC010000	-2.46	0.0028	Wnt9a	Protein Wnt-9a precursor (Wnt-14).
mMR026292	-2.43	0.0107	Nfatc1	Nuclear factor of activated T-cells, cytoplasmic 1.
mMC021250	-2.42	0.0051	Pitx1	Pituitary homeobox 1 (Homeobox protein P-OTX).
mMC016640	-2.4	0.0388	Pola1	DNA polymerase alpha catalytic subunit.
mMC016646	-2.39	0.0067	Egfr	Epidermal growth factor receptor precursor.
mMC009648	-2.39	0.0006	Bmp7	Bone morphogenetic protein 7 precursor.
mMC013663	-2.39	0.0118	Tnmd	Tenomodulin (TeM) (mTeM) (Chondromodulin-I-like protein).
mMC003890	-2.38	0.0064	Crabp2	Cellular retinoic acid-binding protein 2.
mMC008043	-2.37	0.0204	Chek1	Serine/threonine-protein kinase Chk1.
mMC004121	-2.36	0.0066	Spc24	Kinetochore protein Spc24.
mMR029934	-2.35	0.0017	Cdc6	Cell division control protein 6 homolog.
mMR029574	-2.33	0.0004	Bmpr1b	Bone morphogenetic protein receptor type IB precursor.
mMC002759	-2.31	0.027	Rad51	DNA repair protein RAD51 homolog 1.
mMC010318	-2.31	0.0165	Foxd1	Forkhead box protein D1.
mMC008299	-2.31	0.0111	Efemp1	EGF-containing fibulin-like extracellular matrix protein 1.
mMC019230	-2.29	0.0291	Tbx15	T-box transcription factor TBX15.
mMC005043	-2.29	0.0052	Twist1	Twist-related protein 1 (M-twist).
mMR027407	-2.28	0.0203	Ddx3y	ATP-dependent RNA helicase DDX3Y.
mMC004631	-2.27	0.0059	Lmcd1	LIM and cysteine-rich domains protein 1.
mMC025368	-2.27	0.0022	Cdc20	Cell division cycle protein 20 homolog.

mMC023569	-2.26	0.0074	Cdc6	Cell division control protein 6 homolog.
mMR028442	-2.26	0.0331	Dtl	Denticleless protein homolog.
mMC022184	-2.26	0.0013	Gtse1	G2 and S phase-expressed protein 1.
mMR028305	-2.24	0.0155	Lhx8	LIM/homeobox protein Lhx8.

probe id	<i>Bmp4</i> OE vs Control (FoldChange)	<i>Bmp4</i> OE vs Control (Pvalue)	Ensembl Gene Symbol	Ensembl Gene Description
mMC018720	-2.24	0.0006	Eya2	Eyes absent homolog 2.
mMC020210	-2.23	0.0025	Spon1	Spondin-1 precursor (F-spondin).
mMC010627	-2.22	0.0124	Gbx2	Gastrulation and brain-specific homeobox protein 2.
mMC018217	-2.22	0.0063	Cenpn	Centromere protein N (CENP-N).
mMC006090	-2.22	0.0319	Wbp11	WW domain-binding protein 11 (WBP-11).
mMC003963	-2.21	0.0163	Fap	Seprase (Fibroblast activation protein alpha).
mMC010387	-2.2	0.025	Spry2	Protein sprouty homolog 2.
mMC006225	-2.2	0.0012	Aurka	Serine/threonine-protein kinase 6 (Aurora kinase A).
mMC022453	-2.19	0.0265	Fgf10	Fibroblast growth factor 10 precursor.
mMC012277	-2.19	0.0462	Mns1	Meiosis-specific nuclear structural protein 1.
mMC006899	-2.18	0.0384	Brca1	Breast cancer type 1 susceptibility protein homolog.
mMR029214	-2.18	0.0297	Smc2	Structural maintenance of chromosomes protein 2.
mMC022196	-2.18	0.0039	Col23a1	Collagen alpha-1(XXIII) chain.
mMC014446	-2.17	0.043	Incenp	Inner centromere protein.
mMC006074	-2.16	0.0034	Xrcc3	X-ray repair cross-complementing protein 3.
mMC014443	-2.15	0.0033	Cdc25c	M-phase inducer phosphatase 3.
mMR028076	-2.15	0.007	Barx2	Homeobox protein BarH-like 2.
mMC016874	-2.14	0.0018	Sgol2	Shugoshin-like 2.
mMC012062	-2.14	0.0075	Hist1h2ao	Histone H2A type 1.
mMC009891	-2.13	0.0012	Spc25	Kinetochore protein Spc25.
mMC017517	-2.13	0.0049	Mlf1	Myeloid leukemia factor 1.
mMC009710	-2.13	0.035	Bard1	BRCA1-associated RING domain protein 1 (BARD-1).
mMC014769	-2.13	0.0117	Rarb	Retinoic acid receptor beta (RAR-beta).
mMC007490	-2.11	0.0023	Dcp2	mRNA-decapping enzyme 2.
mMC003317	-2.11	0.0287	Ercc6l	excision repair cross-complementing group 6 - like.
mMR030048	-2.11	0.008	Wnt5a	Protein Wnt-5a precursor.
mMC006771	-2.11	0.0115	Eml3	Echinoderm microtubule-associated protein-like 3 (EMAP-3).
mMC007743	-2.11	0.0096	Ccnb2	G2/mitotic-specific cyclin-B2.
mMC014831	-2.1	0.0026	Hist1h1b	Histone H1.5 (H1 VAR.5) (H1b).
mMR026709	-2.1	0.0277	Mbnl3	Muscleblind-like X-linked protein 3.
mMC017313	-2.1	0.0317	Gas2	Growth arrest-specific protein 2.
mMR028181	-2.09	0.0002	Timp3	Metalloproteinase inhibitor 3 precursor.
mMC002529	-2.08	0.0265	Bcl2	Apoptosis regulator Bcl-2.
mMC011122	-2.08	0.0339	Cebpz	CCAAT/enhancer-binding protein zeta.
mMC022135	-2.08	0.0012	Plk1	Serine/threonine-protein kinase PLK1.
mMC017102	-2.07	0.0205	Cdca2	Cell division cycle-associated protein 2.
mMC022855	-2.07	0.0006	Ccnb1	G2/mitotic-specific cyclin-B1.
mMC014639	-2.05	0.0099	Pold2	DNA polymerase subunit delta-2.
mMC005065	-2.05	0.0194	Rbm8a	RNA-binding protein 8A.
mMC004902	-2.05	0.0254	Pif1	ATP-dependent DNA helicase PIF1.
mMR029647	-2.03	0.0053	Lix1	Protein limb expression 1 homolog.
mMR027721	-2.03	0.0234	Col8a2	Collagen alpha-2(VIII) chain precursor, Endothelial collagen.
mMR028184	-2.03	0.0047	Gas2	Growth arrest-specific protein 2 (GAS-2).
mMC016105	-2.03	0.0381	Six2	Homeobox protein SIX2 (Sine oculis homeobox homolog 2).

mMC018871	-2.01	0.0042	Cenpm	Centromere protein M.
mMC005713	-2.01	0.0377	Cenpf	centromere protein F.
mMR026745	-2.01	0.0026	Tcfap2b	Transcription factor AP-2 beta.
mMC001743	-2	0.0044	Has3	Hyaluronan synthase 3.
mMC026007	-2	0.0099	Suv39h2	Histone-lysine N-methyltransferase SUV39H2.

probe id	<i>Bmp4</i> OE vs Control (FoldChange)	<i>Bmp4</i> OE vs Control (Pvalue)	Gene Symbol	Ensembl_Gene_Description
mMR030652	2	0.0194	Socs2	Suppressor of cytokine signaling 2.
mMC025149	2.01	0.0474	Olfr282	olfactory receptor 282.
mMC007940	2.01	0.0002	Msx1	Homeobox protein MSX-1 (Msh homeobox 1-like protein).
mMC016067	2.02	0.0183	Smyd1	SET and MYND domain-containing protein 1.
mMC014229	2.03	0.0083	Meis2	Homeobox protein Meis2 (Meis1-related protein 1).
mMC011307	2.05	0.0235	Mafb	Transcription factor MafB.
mMC021817	2.05	0.0149	Il18	Interleukin-18 precursor.
mMC014455	2.05	0.0223	Hao3	Hydroxyacid oxidase 2.
mMC024996	2.06	0.0208	Ehmt1	euchromatic histone methyltransferase 1 isoform 1 .
mMC004022	2.06	0.0174	Med17	Mediator of RNA polymerase II transcription subunit 17.
mMC012216	2.07	0.0058	Gpr50	Melatonin-related receptor (G protein-coupled receptor 50).
mMC008429	2.08	0.002	Guca1b	Guanylate cyclase activator 1B.
mMC017691	2.09	0.0123	Tle2	Transducin-like enhancer protein 2.
mMC006701	2.09	0.0489	Olfr552	olfactory receptor 552.
mMC004293	2.09	0.0103	Adh1	Alcohol dehydrogenase 1.
mMC018176	2.1	0.0476	Art2b	T-cell ecto-ADP-ribosyltransferase 2 precursor.
mMR030084	2.1	0.0053	Igfbp5	Insulin-like growth factor-binding protein 5 precursor.
mMC024704	2.11	0.0171	Olfr1102	Olfactory receptor 1102.
mMC006134	2.12	0.0389	Isl2	Insulin gene enhancer protein ISL-2 (Islet-2).
mMC004625	2.12	0.0033	Gpr19	Probable G-protein coupled receptor 19.
mMR029458	2.13	0.0141	Tgfb1i1	Transforming growth factor beta-1-induced transcript 1.
mMC018508	2.13	0.0469	Taok3	Serine/threonine-protein kinase TAO3.
mMC006059	2.13	0.024	Spink5	serine peptidase inhibitor, Kazal type 5.
mMR027435	2.13	0.0047	Col24a1	procollagen, type XXIV, alpha 1.
mMC012387	2.13	0.0129	Tle6	Transducin-like enhancer protein 6.
mMR030613	2.14	0.0234	Gria2	Glutamate receptor 2 precursor.
mMC018518	2.14	0.042	Gprc5d	G-protein coupled receptor family C group 5 member D.
mMC005104	2.15	0.0051	Sox5	Transcription factor SOX-5.
mMC001008	2.16	0.0215	Efna1	Ephrin-A1 (EPH-related receptor tyrosine kinase ligand 1).
mMC012578	2.16	0.0219	Hspa2	Heat shock-related 70 kDa protein 2.
mMC018772	2.17	0.0002	Gprin3	G protein-regulated inducer of neurite outgrowth 3.
mMC022310	2.19	0.0265	Pafah1b2	Platelet-activating factor acetylhydrolase IB subunit beta.
mMC025035	2.19	0.0133	Elmo1	Engulfment and cell motility protein 1 (CED-12 homolog).
mMC002788	2.21	0.025	Msr2	macrophage scavenger receptor 2.
mMR028041	2.22	0.0089	Serf1	Small EDRK-rich factor 1 (4F5) (m4F5).
mMC007974	2.23	0.0252	Spsb1	SPRY domain-containing SOCS box protein 1 (SSB-1).
mMC025800	2.24	0.0004	Unc13b	Protein unc-13 homolog B (Munc13-2).
mMC003788	2.24	0.0036	Prrx2	Paired mesoderm homeobox protein 2.
mMC008313	2.24	0.0275	Map3k1	Mitogen-activated protein kinase kinase kinase 1.
mMR030964	2.24	0.0286	Ptgs2	Prostaglandin G/H synthase 2 precursor.

probe id	<i>Bmp4</i> OE vs Control (FoldChange)	<i>Bmp4</i> OE vs Control (Pvalue)	Gene Symbol	Ensembl_Gene_Description
mMC019189	2.25	0.0051	Olf459	olfactory receptor 459.
mMR028863	2.25	0.0015	Klf5	Krueppel-like factor 5.
mMC018573	2.26	0.0378	Olf411	olfactory receptor 411.
mMR030035	2.26	0.0096	Satb1	Special AT-rich sequence-binding protein 1.
mMC013645	2.26	0.0033	Alcam	CD166 antigen precursor.
mMC023971	2.28	0.0203	Pmp22	Peripheral myelin protein 22.
mMC007194	2.3	0.0177	Cd1d1	T-cell surface glycoprotein CD1d1 precursor.
mMC004741	2.31	0.0033	Skil	Ski-like protein.
mMC009330	2.31	0.0366	Olf651	olfactory receptor 651.
mMC007674	2.32	0.0198	Mypn	Myopalladin.
mMC021286	2.34	0.0188	Actg1	Actin, cytoplasmic 2 (Gamma-actin).
mMC020398	2.34	0.0064	Krt8	Keratin, type II cytoskeletal 8.
mMC006869	2.36	0.0315	Spon2	Spondin-2 precursor (Mandin).
mMR029558	2.39	0.0045	Rgs2	Regulator of G-protein signaling 2 (RGS2).
mMC019522	2.44	0.0356	Shroom1	Protein Shroom1.
mMC014141	2.44	0.0378	Olf123	olfactory receptor 123.
mMR031232	2.44	0.001	Cux2	Homeobox protein cut-like 2.
mMC000927	2.45	0.0395	Derl1	Degradation in endoplasmic reticulum protein 1.
mMC004037	2.46	0.003	Angpt2	Angiopoietin-2 precursor.
mMC010754	2.46	0.0229	Abca1	ATP-binding cassette sub-family A member 1.
mMR027525	2.48	0.0067	Bmf	Bcl-2-modifying factor.
mMC025342	2.48	0.0176	Syp	Synaptophysin (Major synaptic vesicle protein p38).
mMC014959	2.49	0.0257	Id1	DNA-binding protein inhibitor, Inhibitor of DNA binding 1.
mMR030256	2.5	0.0119	Evi1	Ecotropic virus integration site 1 protein.
mMC023884	2.53	0.0392	Icos	Inducible T-cell co-stimulator precursor.
mMC011878	2.53	0.0329	Nrtm	Neurturin precursor.
mMC002262	2.53	0.0203	Tnnt1	Troponin T, slow skeletal muscle.
mMC004603	2.55	0.0216	Pdlim3	PDZ and LIM domain protein 3.
mMR029853	2.59	0.0046	Sox5	Transcription factor SOX-5.
mMC015376	2.6	0.0122	Lgals3	Galectin-3 (Galactose-specific lectin 3).
mMC025896	2.6	0.0032	Dbx1	Developing brain homeobox protein 1.
mMC008166	2.61	0.0101	Olf740	olfactory receptor 740
mMC012597	2.62	0.0461	Nfkb1a	NF-kappa-B inhibitor alpha (I-kappa-B-alpha).
mMC018691	2.62	0.0008	Dck	Deoxycytidine kinase.
mMC004630	2.64	0.0006	Yipf2	Protein YIPF2 (YIP1 family member 2).
mMC015898	2.64	0.0002	Dkk1	Dickkopf-related protein 1 precursor.
mMC001101	2.65	0.0266	Plac8	Placenta-specific gene 8 protein.
mMC009367	2.65	0.0019	Atf3	Cyclic AMP-dependent transcription factor ATF-3.
mMC007158	2.66	0.0021	Zfp2	Zinc finger protein ZFP2 (Friend of GATA protein 2).

probe id	<i>Bmp4</i> OE vs Control (FoldChange)	<i>Bmp4</i> OE vs Control (Pvalue)	Gene Symbol	Ensembl Gene Description
mMC001049	2.7	0.0047	Thbs3	Thrombospondin-3 precursor.
mMC018723	2.77	0.004	Epyc	Epiphykan precursor (Dermatan sulfate proteoglycan 3).
mMR030076	2.84	0.0063	Klf3	Krueppel-like factor 3.
mMC012911	2.91	0.0019	Sox5	Transcription factor SOX-5.
mMC008743	2.94	0.0169	Olfr1428	olfactory receptor 1428.
mMC002022	2.96	0.0046	Vsx1	Visual system homeobox 1.
mMC004722	2.97	0.0173	Olfr1423	olfactory receptor 1423.
mMC005384	3.06	0.0204	Sepp1	Selenoprotein P precursor.
mMC021603	3.06	0.0056	Fgf22	Fibroblast growth factor 22 precursor.
mMC013726	3.16	0.0165	Nkx2-6	Homeobox protein Nkx-2.6.
mMC004723	3.21	0.0015	Kap	Kidney androgen-regulated protein precursor.
mMC006543	3.24	0.0072	Olfr571	olfactory receptor 571.
mMC006067	3.31	0.0028	Msx2	Homeobox protein MSX-2 (Hox-8.1).
mMC012563	3.32	0.0038	Gadd45g	Growth arrest and DNA-damage-inducible protein.
mMC011946	3.51	0.0272	Eid1	EP300-interacting inhibitor of differentiation 1.
mMC008354	3.59	0.0032	Sox8	Transcription factor SOX-8.
mMC006928	3.63	0.0306	Actr1	Actin-related protein T1.
mMC007645	3.71	0.001	Bmf	Bcl-2-modifying factor.
mMC019148	3.75	0.0028	Col9a2	Collagen alpha-2(IX) chain precursor.
mMC007751	3.84	0.0002	Hand1	Heart- and neural crest derivatives-expressed protein 1.
mMC011983	3.9	0.0108	Odf1	Outer dense fiber protein 1.
mMR028115	3.91	0.0027	Ntn1	Netrin-G1 precursor (Lamint-1).
mMR029269	4.04	0.0007	Col9a1	Collagen alpha-1(IX) chain precursor.
mMC002384	4.15	0.0022	Gadd45b	Growth arrest and DNA-damage-inducible protein.
mMC005244	4.24	0.0053	S100a8	S100 calcium-binding protein A8 (Calgranulin-A).
mMC009186	4.26	0.0034	Tbx20	T-box transcription factor TBX20.
mMC023939	4.43	0.0019	Gata6	Transcription factor GATA-6 (GATA-binding factor 6).
mMC011282	4.46	0.0053	Fbxo2	F-box only protein 2.
mMC012619	4.59	0.0052	Nog	Noggin precursor.
mMC008700	5.25	0.0003	Smad6	Mothers against decapentaplegic homolog 6.
mMC008103	5.42	0.0002	Col9a3	procollagen, type IX, alpha 3.
mMC020041	5.53	0.0022	Unc5b	Netrin receptor UNC5B precursor.
mMC005675	5.58	0.01	Angpt1	Angiotensinogen-1 precursor (ANG-1).
mMR029110	5.63	0.0005	Pdgfrl	Platelet-derived growth factor receptor-like protein.
mMC013000	6.25	0.0026	Gata2	Endothelial transcription factor GATA-2.
mMC002592	7.32	0.0017	Igf1	Insulin-like growth factor-binding protein 7 precursor.
mMC008257	7.74	0.0013	Rgs5	Regulator of G-protein signaling 5.
mMC013455	7.89	6.84E-05	Isl1	Insulin gene enhancer protein ISL-1.
mMC017480	9.68	0.0003	Bmp4	Bone morphogenetic protein 4 precursor.
mMC021077	12.47	0.0031	Gata3	Trans-acting T-cell-specific transcription factor GATA-3.
mMC007167	12.97	6.69E-05	Sct	Secretin precursor.

Bibliography

Abzhanov, A., Protas, M., Grant, B. R., Grant, P. R. and Tabin, C. J. (2004). Bmp4 and morphological variation of beaks in Darwin's finches. *Science* **305**, 1462-5.

Albertson, R. C., Streelman, J. T., Kocher, T. D. and Yelick, P. C. (2005). Integration and evolution of the cichlid mandible: the molecular basis of alternate feeding strategies. *Proc Natl Acad Sci U S A* **102**, 16287-92.

Barbosa, A. C., Funato, N., Chapman, S., McKee, M. D., Richardson, J. A., Olson, E. N. and Yanagisawa, H. (2007). Hand transcription factors cooperatively regulate development of the distal midline mesenchyme. *Dev Biol* **310**, 154-68.

Bartel, D. P. (2009). MicroRNAs: target recognition and regulatory functions. *Cell* **136**, 215-33.

Belteki, G., Haigh, J., Kabacs, N., Haigh, K., Sison, K., Costantini, F., Whitsett, J., Quaggin, S. E. and Nagy, A. (2005). Conditional and inducible transgene expression in mice through the combinatorial use of Cre-mediated recombination and tetracycline induction. *Nucleic Acids Res* **33**, e51.

Britanova, O., Depew, M. J., Schwark, M., Thomas, B. L., Miletich, I., Sharpe, P. and Tarabykin, V. (2006). Satb2 haploinsufficiency phenocopies 2q32-q33

deletions, whereas loss suggests a fundamental role in the coordination of jaw development. *Am J Hum Genet* **79**, 668-78.

Brunet, L. J., McMahon, J. A., McMahon, A. P. and Harland, R. M. (1998). Noggin, cartilage morphogenesis, and joint formation in the mammalian skeleton [see comments]. *Science* **280**, 1455-7.

Chai, Y., Jiang, X., Ito, Y., Bringas, P., Han, J., Rowitch, D. H., Soriano, P., McMahon, A. P. and Sucov, H. M. (2000). Fate of the mammalian cranial neural crest during tooth and mandibular morphogenesis. *Development* **127**, 1671-9.

Chai, Y. and Maxson, R. E., Jr. (2006). Recent advances in craniofacial morphogenesis. *Dev Dyn* **235**, 2353-75.

Charite, J., McFadden, D. G., Merlo, G., Levi, G., Clouthier, D. E., Yanagisawa, M., Richardson, J. A. and Olson, E. N. (2001). Role of Dlx6 in regulation of an endothelin-1-dependent, dHAND branchial arch enhancer. *Genes Dev* **15**, 3039-49.

Chen, R. M., Lin, Y. L. and Chou, C. W. (2010). GATA-3 transduces survival signals in osteoblasts through upregulation of bcl-x(L) gene expression. *J Bone Miner Res* **25**, 2193-204.

Chen, X., Xu, H., Yuan, P., Fang, F., Huss, M., Vega, V. B., Wong, E., Orlov, Y. L., Zhang, W., Jiang, J., Loh, Y. H., Yeo, H. C., Yeo, Z. X., Narang, V., Govindarajan, K. R., Leong, B., Shahab, A., Ruan, Y., Bourque, G., Sung, W. K., Clarke, N. D., Wei, C. L. and Ng, H. H. (2008). Integration of external signaling

pathways with the core transcriptional network in embryonic stem cells. *Cell* **133**, 1106-17.

Choi, M., Stottmann, R. W., Yang, Y. P., Meyers, E. N. and Klingensmith, J. (2007). The bone morphogenetic protein antagonist noggin regulates mammalian cardiac morphogenesis. *Circ Res* **100**, 220-8.

Davis, B. N., Hilyard, A. C., Lagna, G. and Hata, A. (2008). SMAD proteins control DROSHA-mediated microRNA maturation. *Nature* **454**, 56-61.

Depew, M. J., Lufkin, T. and Rubenstein, J. L. (2002). Specification of jaw subdivisions by Dlx genes. *Science* **298**, 381-5.

Dobrev, G., Chahrour, M., Dautzenberg, M., Chirivella, L., Kanzler, B., Farinas, I., Karsenty, G. and Grosschedl, R. (2006). SATB2 is a multifunctional determinant of craniofacial patterning and osteoblast differentiation. *Cell* **125**, 971-86.

Fei, T., Xia, K., Li, Z., Zhou, B., Zhu, S., Chen, H., Zhang, J., Chen, Z., Xiao, H., Han, J. D. and Chen, Y. G. (2010). Genome-wide mapping of SMAD target genes reveals the role of BMP signaling in embryonic stem cell fate determination. *Genome Res* **20**, 36-44.

Funato, N., Chapman, S. L., McKee, M. D., Funato, H., Morris, J. A., Shelton, J. M., Richardson, J. A. and Yanagisawa, H. (2009). Hand2 controls osteoblast differentiation in the branchial arch by inhibiting DNA binding of Runx2. *Development* **136**, 615-25.

Gitton, Y., Heude, E., Vieux-Rochas, M., Benouaiche, L., Fontaine, A., Sato, T., Kurihara, Y., Kurihara, H., Couly, G. and Levi, G. (2010). Evolving maps in craniofacial development. *Semin Cell Dev Biol* **21**, 301-8.

Gong, Y., Krakow, D., Marcelino, J., Wilkin, D., Chitayat, D., Babul-Hirji, R., Hudgins, L., Cremers, C. W., Cremers, F. P., Brunner, H. G., Reinker, K., Rimoin, D. L., Cohn, D. H., Goodman, F. R., Reardon, W., Patton, M., Francomano, C. A. and Warman, M. L. (1999). Heterozygous mutations in the gene encoding noggin affect human joint morphogenesis. *Nat Genet* **21**, 302-4.

Gossen, M., Freundlieb, S., Bender, G., Muller, G., Hillen, W. and Bujard, H. (1995). Transcriptional activation by tetracyclines in mammalian cells. *Science* **268**, 1766-9.

Graham, A., Begbie, J. and McGonnell, I. (2004). Significance of the cranial neural crest. *Dev Dyn* **229**, 5-13.

He, F., Xiong, W., Wang, Y., Matsui, M., Yu, X., Chai, Y., Klingensmith, J. and Chen, Y. (2010). Modulation of BMP signaling by Noggin is required for the maintenance of palatal epithelial integrity during palatogenesis. *Dev Biol* **347**, 109-21.

Ishii, M., Han, J., Yen, H. Y., Sucov, H. M., Chai, Y. and Maxson, R. E., Jr. (2005). Combined deficiencies of Msx1 and Msx2 cause impaired patterning and survival of the cranial neural crest. *Development* **132**, 4937-50.

Ishii, M., Merrill, A. E., Chan, Y. S., Gitelman, I., Rice, D. P., Sucov, H. M. and Maxson, R. E., Jr. (2003). Msx2 and Twist cooperatively control the development of the neural crest-derived skeletogenic mesenchyme of the murine skull vault. *Development* **130**, 6131-42.

Iulianella, A., Sharma, M., Vanden Heuvel, G. B. and Trainor, P. A. (2009). Cux2 functions downstream of Notch signaling to regulate dorsal interneuron formation in the spinal cord. *Development* **136**, 2329-34.

Iulianella, A., Vanden Heuvel, G. and Trainor, P. (2003). Dynamic expression of murine Cux2 in craniofacial, limb, urogenital and neuronal primordia. *Gene Expr Patterns* **3**, 571-7.

Jiang, X., Iseki, S., Maxson, R. E., Sucov, H. M. and Morriss-Kay, G. M. (2002). Tissue origins and interactions in the mammalian skull vault. *Dev Biol* **241**, 106-16.

Kanzler, B., Foreman, R. K., Labosky, P. A. and Mallo, M. (2000). BMP signaling is essential for development of skeletogenic and neurogenic cranial neural crest. *Development* **127**, 1095-104.

Kirilly, D., Spana, E. P., Perrimon, N., Padgett, R. W. and Xie, T. (2005). BMP signaling is required for controlling somatic stem cell self-renewal in the *Drosophila* ovary. *Dev Cell* **9**, 651-62.

Knecht, A. K. and Bronner-Fraser, M. (2002). Induction of the neural crest: a multigene process. *Nat Rev Genet* **3**, 453-61.

Korchynskyi, O. and ten Dijke, P. (2002). Identification and functional characterization of distinct critically important bone morphogenetic protein-specific response elements in the Id1 promoter. *J Biol Chem* **277**, 4883-91.

Liu, W., Selever, J., Murali, D., Sun, X., Brugger, S. M., Ma, L., Schwartz, R. J., Maxson, R., Furuta, Y. and Martin, J. F. (2005a). Threshold-specific requirements for Bmp4 in mandibular development. *Dev Biol* **283**, 282-93.

Liu, W., Selever, J., Wang, D., Lu, M. F., Moses, K. A., Schwartz, R. J. and Martin, J. F. (2004). Bmp4 signaling is required for outflow-tract septation and branchial-arch artery remodeling. *Proc Natl Acad Sci U S A* **101**, 4489-94.

Liu, W., Sun, X., Braut, A., Mishina, Y., Behringer, R. R., Mina, M. and Martin, J. F. (2005b). Distinct functions for Bmp signaling in lip and palate fusion in mice. *Development* **132**, 1453-1461.

Ma, L., Lu, M. F., Schwartz, R. J. and Martin, J. F. (2005). Bmp2 is essential for cardiac cushion epithelial-mesenchymal transition and myocardial patterning. *Development* **132**, 5601-11.

Massague, J., Seoane, J. and Wotton, D. (2005). Smad transcription factors. *Genes Dev* **19**, 2783-810.

McFadden, D. G., Barbosa, A. C., Richardson, J. A., Schneider, M. D., Srivastava, D. and Olson, E. N. (2005). The Hand1 and Hand2 transcription factors regulate expansion of the embryonic cardiac ventricles in a gene dosage-dependent manner. *Development* **132**, 189-201.

- Merrill, A. E., Eames, B. F., Weston, S. J., Heath, T. and Schneider, R. A.** (2008). Mesenchyme-dependent BMP signaling directs the timing of mandibular osteogenesis. *Development* **135**, 1223-34.
- Mitsiadis, T. A., Angeli, I., James, C., Lendahl, U. and Sharpe, P. T.** (2003). Role of Islet1 in the patterning of murine dentition. *Development* **130**, 4451-60.
- Nie, X., Luukko, K. and Kettunen, P.** (2006). BMP signalling in craniofacial development. *Int J Dev Biol* **50**, 511-21.
- Noden, D. M. and Trainor, P. A.** (2005). Relations and interactions between cranial mesoderm and neural crest populations. *J Anat* **207**, 575-601.
- Nohe, A., Keating, E., Knaus, P. and Petersen, N. O.** (2004). Signal transduction of bone morphogenetic protein receptors. *Cell Signal* **16**, 291-9.
- Paulsen, M., Legewie, S., Eils, R., Karaulanov, E. and Niehrs, C.** (2011). Negative feedback in the bone morphogenetic protein 4 (BMP4) synexpression group governs its dynamic signaling range and canalizes development. *Proc Natl Acad Sci U S A* **108**, 10202-7.
- Potvin, E., Beuret, L., Cadrin-Girard, J. F., Carter, M., Roy, S., Tremblay, M. and Charron, J.** (2010). Cooperative action of multiple cis-acting elements is required for N-myc expression in branchial arches: specific contribution of GATA3. *Mol Cell Biol* **30**, 5348-63.

Prall, O. W., Menon, M. K., Solloway, M. J., Watanabe, Y., Zaffran, S., Bajolle, F., Biben, C., McBride, J. J., Robertson, B. R., Chaulet, H., Stennard, F. A., Wise, N., Schaft, D., Wolstein, O., Furtado, M. B., Shiratori, H., Chien, K. R., Hamada, H., Black, B. L., Saga, K., Robertson, E. J., Buckingham, M. E. and Harvey, R. P. (2007). An Nkx2-5/Bmp2/Smad1 negative feedback loop controls heart progenitor specification and proliferation. *Cell* **128**, 947-59.

Ralston, A., Cox, B. J., Nishioka, N., Sasaki, H., Chea, E., Rugg-Gunn, P., Guo, G., Robson, P., Draper, J. S. and Rossant, J. (2010). Gata3 regulates trophoblast development downstream of Tead4 and in parallel to Cdx2. *Development* **137**, 395-403.

Ruest, L.-B., Xiang, X., Lim, K.-C., Levi, G. and Clouthier, D. E. (2004a). Endothelin A receptor-dependent and independent signaling pathways in establishing mandibular identity. *Development* **131**, 4413-4423.

Ruest, L. B., Xiang, X., Lim, K. C., Levi, G. and Clouthier, D. E. (2004b). Endothelin-A receptor-dependent and -independent signaling pathways in establishing mandibular identity. *Development* **131**, 4413-23.

Shen, T., Aneas, I., Sakabe, N., Dirschinger, R. J., Wang, G., Smemo, S., Westlund, J. M., Cheng, H., Dalton, N., Gu, Y., Boogerd, C., Cai, C. L., Peterson, K., Chen, J., Nobrega, M. and Evans, S. (2011). Tbx20 regulates a genetic program essential to adult mouse cardiomyocyte function. *J Clin Invest* **121**, 4640-54.

Sheng, N., Xie, Z., Wang, C., Bai, G., Zhang, K., Zhu, Q., Song, J., Guillemot, F., Chen, Y. G., Lin, A. and Jing, N. (2010). Retinoic acid regulates bone morphogenic protein signal duration by promoting the degradation of phosphorylated Smad1. *Proc Natl Acad Sci U S A* **107**, 18886-91.

Shin, M. K., Levorse, J. M., Ingram, R. S. and Tilghman, S. M. (1999). The temporal requirement for endothelin receptor-B signalling during neural crest development. *Nature* **402**, 496-501.

Suzuki, S., Marazita, M. L., Cooper, M. E., Miwa, N., Hing, A., Jugessur, A., Natsume, N., Shimosato, K., Ohbayashi, N., Suzuki, Y., Niimi, T., Minami, K., Yamamoto, M., Altannamar, T. J., Erkhembaatar, T., Furukawa, H., Daack-Hirsch, S., L'Heureux, J., Brandon, C. A., Weinberg, S. M., Neiswanger, K., Deleyiannis, F. W. B., de Salamanca, J. E., Vieira, A. R., Lidral, A. C., Martin, J. F. and Murray, J. C. (2009). Mutations in BMP4 are associated with subepithelial, microform, and overt cleft lip. *Am J Hum Genet* **84**, 406-11.

Tribulo, C., Aybar, M. J., Nguyen, V. H., Mullins, M. C. and Mayor, R. (2003). Regulation of Msx genes by a Bmp gradient is essential for neural crest specification. *Development* **130**, 6441-52.

Tsarovina, K., Reiff, T., Stubbusch, J., Kurek, D., Grosveld, F. G., Parlato, R., Schutz, G. and Rohrer, H. (2010). The Gata3 transcription factor is required for the survival of embryonic and adult sympathetic neurons. *J Neurosci* **30**, 10833-43.

Wang, J., Greene, S. B., Bonilla-Claudio, M., Tao, Y., Zhang, J., Bai, Y., Huang, Z., Black, B. L., Wang, F. and Martin, J. F. (2010). Bmp signaling regulates myocardial differentiation from cardiac progenitors through a MicroRNA-mediated mechanism. *Dev Cell* **19**, 903-12.

Wang, J., Greene, S. B. and Martin, J. F. (2011). BMP signaling in congenital heart disease: new developments and future directions. *Birth Defects Res A Clin Mol Teratol* **91**, 441-8.

Wu, P., Jiang, T. X., Suksaweang, S., Widelitz, R. B. and Chuong, C. M. (2004). Molecular shaping of the beak. *Science* **305**, 1465-6.

Xu, X., Han, J., Ito, Y., Bringas, P., Jr., Deng, C. and Chai, Y. (2008). Ectodermal Smad4 and p38 MAPK are functionally redundant in mediating TGF-beta/BMP signaling during tooth and palate development. *Dev Cell* **15**, 322-9.

Ying, Q. L., Nichols, J., Chambers, I. and Smith, A. (2003). BMP induction of Id proteins suppresses differentiation and sustains embryonic stem cell self-renewal in collaboration with STAT3. *Cell* **115**, 281-92.

Zhang, P., Andrianakos, R., Yang, Y., Liu, C. and Lu, W. (2010). Kruppel-like factor 4 (Klf4) prevents embryonic stem (ES) cell differentiation by regulating Nanog gene expression. *J Biol Chem* **285**, 9180-9.

Vita

Margarita Bonilla-Claudio was born in Caguas, Puerto Rico on August 14, 1981. She is the third of four sons of Porfirio Bonilla-Santa and Nancy M. Claudio-Ramos. After completing her studies at Dra. Conchita Cuevas High School, Gurabo, Puerto Rico in 1999, she entered the University of Puerto Rico at Cayey in Cayey, Puerto Rico, where she received the degree of Bachelor of Science *Magna Cum Laude* in May, 2004, with a major in Biology. In September of 2004, she entered The University of Texas Health Science Center Graduate School of Biomedical Sciences at Houston. After completing research tutorials, she joined the laboratory of Dr. James F. Martin and the Genes and Development Program in June, 2005.